Electronic Supplementary Material (ESI) for Journal of Materials Chemistry A.

Electronic Supplementary Information

Acetylene-linked conjugated polymers for sacrificial photocatalytic hydrogen evolution from water

Lunjie Liu,[a] Michał Andrzej Kochman,[b] Yongjie Xu,[a] Martijn A. Zwijnenburg,*[,b] Andrew I. Cooper*[,a] and Reiner Sebastian Sprick*[,a,c]

[a] Department of Chemistry and Materials Innovation Factory, University of Liverpool, 51 Oxford Street, Liverpool L7 3NY, U.K.

[b] Department of Chemistry, University College London, 20 Gordon Street, London WC1H 0AJ, U.K.

[c] Department of Pure and Applied Chemistry, University of Strathclyde, Thomas Graham Building, 295 Cathedral Street, Glasgow G1 1XL, U.K.

[*] Corresponding authors: m.zwijnenburg@ucl.ac.uk (M.A.Z.), aicooper@liverpool.ac.uk (A.I.C.), sebastian.sprick@strath.ac.uk (R.S.S.).

1 Polymer synthesis results

TE1: 2,5-Dibromothiophene (242 mg, 1 mmol), 1,3,5-triethynylbenzene (100 mg, 0.68 mmol), [$Pd(PPh_3)_2Cl_2$] (18 mg, 0.03 mmol), CuI (10 mg, 0.05 mmol), triphenylphosphine (13 mg, 0.05 mmol), *N*,*N*-dimethylformamide (9 mL) and triethylamine (9 mL) were used in this polycondensation reaction described in the general procedure. After work-up and Soxhlet the product was obtained as a red solid (149.6 mg, 83%). Anal. Calcd for $(C_{12}H_4S)_n$: C, 79.97; H, 2.24; S, 17.79%; Found C, 75.50; H, 3.00; S, 15.50%. Pd content: 1.27%, Cu content: 0.04%.

TE2: 5,5'-Dibromo-2,2'-bithiophene (324 mg, 1 mmol), 1,3,5-triethynylbenzene (100 mg, 0.68 mmol), [$Pd(PPh_3)_2Cl_2$] (18 mg, 0.03 mmol), CuI (10 mg, 0.05 mmol), triphenylphosphine (13 mg, 0.05 mmol), *N*,*N*-dimethylformamide (9 mL) and triethylamine (9 mL) were used in this polycondensation reaction described in the general procedure. After work-up and Soxhlet the product was obtained as a red solid (239.8 mg, 91%). Anal. Calcd for $(C_{16}H_6S_2)_n$: C, 73.25; H, 2.31; S, 24.44%; Found C, 71.00; H, 3.00;S, 23.00%. Pd content: 0.31%, Cu content: 0.02%.

TE3: 5,5''-Dibromo-2,2':5',2''-terthiophene (406 mg, 1 mmol), 1,3,5-triethynylbenzene (100 mg, 0.68 mmol), [$Pd(PPh_3)_2Cl_2$] (18 mg, 0.03 mmol), CuI (10 mg, 0.05 mmol), triphenylphosphine (13 mg, 0.05 mmol), *N*,*N*-dimethylformamide (9 mL) and triethylamine (9 mL) were used in this polycondensation reaction described in the general procedure. After work-up and Soxhlet the product was obtained as a red solid (319.7 mg, 93%). Anal. Calcd for $(C_{20}H_8S_3)_n$: C, 69.74; H, 2.34; S, 27.92%; Found C, 68.00; H, 3.00; S, 26.00%. Pd content: 0.40%, Cu content: 0.00%.

TE4: 2,5-Dibromothieno[3,2-*b*]thiophene (298 mg, 1 mmol), 1,3,5-triethynylbenzene (100 mg, 0.68 mmol), [$Pd(PPh_3)_2Cl_2$] (18 mg, 0.03 mmol), CuI (10 mg, 0.05 mmol), triphenylphosphine (13 mg, 0.05 mmol), *N*,*N*-dimethylformamide (9 mL) and triethylamine (9 mL) were used in this polycondensation reaction described in the general procedure. After work-up and Soxhlet the product was obtained as a red solid (163.4 mg, 69%). Anal. Calcd for $(C_{14}H_4S_2)_n$: C, 71.16; H, 1.71;S, 27.13%; Found C, 65.50; H, 2.00;S, 22.50%. Pd content: 0.99%, Cu content: 0.08%.

TE5: 2,5-Dibromopyrazine (238 mg, 1 mmol), 1,3,5-triethynylbenzene (100 mg, 0.68 mmol), [$Pd(PPh_3)_2Cl_2$] (18 mg, 0.03 mmol), CuI (10 mg, 0.05 mmol), triphenylphosphine (13 mg,

0.05 mmol), *N*,*N*-dimethylformamide (9 mL) and triethylamine (9 mL) were used in this polycondensation reaction described in the general procedure. After work-up and Soxhlet the product was obtained as a yellow solid (146.6 mg, 83%). Anal. Calcd for $(C_{12}H_4N_2)_n$: C, 81.81; H, 2.29; N, 15.90%; Found C, 69.34; H, 2.48; N, 13.20%. Pd content: 1.50%, Cu content: 0.19%.

TE6: 2,5-Dibromopyrimidine (238 mg, 1 mmol), 1,3,5-triethynylbenzene (100 mg, 0.68 mmol), $[Pd(PPh_3)_2Cl_2]$ (18 mg, 0.03 mmol), CuI (10 mg, 0.05 mmol), triphenylphosphine (13 mg, 0.05 mmol), *N*,*N*-dimethylformamide (9 mL) and triethylamine (9 mL) were used in this polycondensation reaction described in the general procedure. After work-up and Soxhlet the product was obtained as a yellow solid (168.4 mg, 96%). Anal. Calcd for $(C_{12}H_4N_2)_n$: C, 81.81; H, 2.29; N, 15.90%; Found C, 69.35; H, 2.51; N, 12.69%. Pd content: 1.10%, Cu content: 0.21%.

TE7: 2,5-Dibromopyridine (237 mg, 1 mmol), 1,3,5-triethynylbenzene (100 mg, 0.68 mmol), $[Pd(PPh_3)_2Cl_2]$ (18 mg, 0.03 mmol), CuI (10 mg, 0.05 mmol), triphenylphosphine (13 mg, 0.05 mmol), *N*,*N*-dimethylformamide (9 mL) and triethylamine (9 mL) were used in this polycondensation reaction described in the general procedure. After work-up and Soxhlet the product was obtained as a yellow solid (154.3 mg, 88%). Anal. Calcd for $(C_{13}H_5N)_n$: C, 89.13; H, 2.88; N, 8.00%; Found C, 74.98; H, 2.77; N, 6.54%. Pd content: 0.11%, Cu content: 0.13%.

TE8: 5,5'-Dibromo-2,2'-bipyridine (314 mg, 1 mmol), 1,3,5-triethynylbenzene (100 mg, 0.68 mmol), $[Pd(PPh_3)_2Cl_2]$ (18 mg, 0.03 mmol), CuI (10 mg, 0.05 mmol), triphenylphosphine (13 mg, 0.05 mmol), *N*,*N*-dimethylformamide (9 mL) and triethylamine (9 mL) were used in this polycondensation reaction described in the general procedure. After work-up and Soxhlet the product was obtained as a yellow solid (116.0 mg, 46%). Anal. Calcd for $(C_{18}H_8N_2)_n$: C, 85.70; H, 3.20; N, 11.10%; Found C, 73.01; H, 2.91; N, 9.33%. Pd content: 0.88%, Cu content: 0.40%.

TE9: 2,7-Dibromofluorene (324 mg, 1 mmol), 1,3,5-triethynylbenzene (100 mg, 0.68 mmol), $[Pd(PPh_3)_2Cl_2]$ (18 mg, 0.03 mmol), CuI (10 mg, 0.05 mmol), triphenylphosphine (13 mg, 0.05 mmol), *N*,*N*-dimethylformamide (9 mL) and triethylamine (9 mL) were used in this polycondensation reaction described in the general procedure. After work-up and Soxhlet the

product was obtained as a yellow solid (251.5 mg, 96%). Anal. Calcd for $(C_{21}H_{10})_n$: C, 96.16; H, 3.84%; Found C, 80.63; H, 3.53%. Pd content: 0.94%, Cu content: 0.11%.

TE10: 3,7-Dibromodibenzo[*b*,*d*]thiophene (342 mg, 1 mmol), 1,3,5-triethynylbenzene (100 mg, 0.68 mmol), $[Pd(PPh_3)_2Cl_2]$ (18 mg, 0.03 mmol), CuI (10 mg, 0.05 mmol), triphenylphosphine (13 mg, 0.05 mmol), *N*,*N*-dimethylformamide (9 mL) and triethylamine (9 mL) were used in this polycondensation reaction described in the general procedure. After work-up and Soxhlet the product was obtained as a yellow solid (262.5 mg, 94%). Anal. Calcd for $(C_{20}H_8S)_n$: C, 85.69; H, 2.88; S, 11.44%; Found C, 73.50; H, 3.00; S, 9.50%. Pd content: 0.59%, Cu content: 0.04%.

TE11: 3,7-Dibromodibenzo[*b*,*d*]thiophene sulfone (374 mg, 1 mmol), 1,3,5-triethynylbenzene (100 mg, 0.68 mmol), $[Pd(PPh_3)_2Cl_2]$ (18 mg, 0.03 mmol), CuI (10 mg, 0.05 mmol), triphenylphosphine (13 mg, 0.05 mmol), *N*,*N*-dimethylformamide (9 mL) and triethylamine (9 mL) were used in this polycondensation reaction described in the general procedure. After work-up and Soxhlet the product was obtained as a yellow solid (291.7 mg, 94%). Anal. Calcd for $(C_{20}H_8O_2S)_n$: C, 76.91; H, 2.58; S, 10.26%; Found C, 69.50; H, 3.00; S, 9.00%. Pd content: 0.64%, Cu content: 0.10%.

TE12: 2,7-Dibromo-9*H*-carbazole (325 mg, 1 mmol), 1,3,5-triethynylbenzene (100 mg, 0.68 mmol), $[Pd(PPh_3)_2Cl_2]$ (18 mg, 0.03 mmol), CuI (10 mg, 0.05 mmol), triphenylphosphine (13 mg, 0.05 mmol), *N*,*N*-dimethylformamide (9 mL) and triethylamine (9 mL) were used in this polycondensation reaction described in the general procedure. After work-up and Soxhlet the product was obtained as a black solid (236.1 mg, 90%). Anal. Calcd for $(C_{20}H_9N)_n$: C, 91.23; H, 3.45; N, 5.32%; Found C, 73.64; H, 3.23; N, 3.40%. Pd content: 0.42%, Cu content: 0.20%.

DE1: 2,5-Dibromothiophene (242 mg, 1 mmol), 1,4-diethynylbenzene (126 mg, 1 mmol), $[Pd(PPh_3)_2Cl_2]$ (18 mg, 0.03 mmol), CuI (10 mg, 0.05 mmol), triphenylphosphine (13 mg, 0.05 mmol), *N*,*N*-dimethylformamide (9 mL) and triethylamine (9 mL) were used in this polycondensation reaction described in the general procedure. After work-up and Soxhlet the product was obtained as a red solid (195.7 mg, 95%). Anal. Calcd for $(C_{14}H_6S)_n$: C, 81.52; H, 2.93; S, 15.54%; Found C, 76.00; H, 3.00; S, 14.00%. Pd content: 0.27%, Cu content: 0.01%.

DE2: 5,5'-Dibromo-2,2'-bithiophene (324 mg, 1 mmol), 1,4-diethynylbenzene (126 mg, 1 mmol), $[Pd(PPh_3)_2Cl_2]$ (18 mg, 0.03 mmol), CuI (10 mg, 0.05 mmol), triphenylphosphine (13 mg, 0.05 mmol), *N*,*N*-dimethylformamide (9 mL) and triethylamine (9 mL) were used in this polycondensation reaction described in the general procedure. After work-up and Soxhlet the product was obtained as a red solid (268.4 mg, 93%). Anal. Calcd for $(C_{18}H_8S_2)_n$: C, 74.97; H, 2.80; S, 22.23%; Found C, 67.00; H, 3.00; S, 20.00%. Pd content: 0.40%, Cu content: 0.02%.

DE3: 5,5''-Dibromo-2,2':5',2''-terthiophene (406 mg, 1 mmol), 1,4-diethynylbenzene (126 mg, 1 mmol), $[Pd(PPh_3)_2Cl_2]$ (18 mg, 0.03 mmol), CuI (10 mg, 0.05 mmol), triphenylphosphine (13 mg, 0.05 mmol), *N*,*N*-dimethylformamide (9 mL) and triethylamine (9 mL) were used in this polycondensation reaction described in the general procedure. After work-up and Soxhlet the product was obtained as a red solid (364.2 mg, 98%). Anal. Calcd for $(C_{22}H_{10}S_3)_n$: C, 71.32; H, 2.72; S, 25.96%; Found C, 64.00; H, 3.50; S, 23.50%. Pd content: 0.45%, Cu content: 0.04%.

DE4: 2,5-Dibromothieno[3,2-*b*]thiophene (298 mg, 1 mmol), 1,4-diethynylbenzene (126 mg, 1 mmol), $[Pd(PPh_3)_2Cl_2]$ (18 mg, 0.03 mmol), CuI (10 mg, 0.05 mmol), triphenylphosphine (13 mg, 0.05 mmol), *N*,*N*-dimethylformamide (9 mL) and triethylamine (9 mL) were used in this polycondensation reaction described in the general procedure. After work-up and Soxhlet the product was obtained as a red solid (250.0 mg, 95%). Anal. Calcd for $(C_{14}H_4S_2)_n$: C, 73.25; H, 2.31; S, 24.44%; Found C, 67.00; H, 3.00; S, 22.50%. Pd content: 0.86%, Cu content: 0.05%.

DE5: 2,5-Dibromopyrazine (238 mg, 1 mmol), 1,4-diethynylbenzene (126 mg, 1 mmol), $[Pd(PPh_3)_2Cl_2]$ (18 mg, 0.03 mmol), CuI (10 mg, 0.05 mmol), triphenylphosphine (13 mg, 0.05 mmol), *N*,*N*-dimethylformamide (9 mL) and triethylamine (9 mL) were used in this polycondensation reaction described in the general procedure. After work-up and Soxhlet the product was obtained as a yellow solid (190.9 mg, 94%). Anal. Calcd for $(C_{14}H_6N_2)_n$: C, 83.16; H, 2.99; N, 13.85%; Found C, 70.87; H, 2.89; N, 11.39%. Pd content: 1.00%, Cu content: 0.09%.

DE6: 2,5-Dibromopyrimidine (238 mg, 1 mmol), 1,4-diethynylbenzene (126 mg, 1 mmol), $[Pd(PPh_3)_2Cl_2]$ (18 mg, 0.03 mmol), CuI (10 mg, 0.05 mmol), triphenylphosphine (13 mg,

0.05 mmol), *N*,*N*-dimethylformamide (9 mL) and triethylamine (9 mL) were used in this polycondensation reaction described in the general procedure. After work-up and Soxhlet the product was obtained as a yellow solid (197.9 mg, 98%). Anal. Calcd for $(C_{14}H_6N_2)_n$: C, 83.16; H, 2.99; N, 13.85%; Found C, 72.07; H, 2.90;N, 11.67%. Pd content: 1.07%, Cu content: 0.05%.

DE7: 2,5-Dibromopyridine (237 mg, 1 mmol), 1,4-diethynylbenzene (126 mg, 1 mmol), $[Pd(PPh_3)_2Cl_2]$ (18 mg, 0.03 mmol), CuI (10 mg, 0.05 mmol), triphenylphosphine (13 mg, 0.05 mmol), *N*,*N*-dimethylformamide (9 mL) and triethylamine (9 mL) were used in this polycondensation reaction described in the general procedure. After work-up and Soxhlet the product was obtained as a yellow solid (194.0 mg, 96%). Anal. Calcd for $(C_{15}H_7N)_n$: C, 89.53; H, 3.51; N, 6.96%; Found C, 76.27; H, 3.23; N, 5.77%. Pd content: 0.43%, Cu content: 0.05%.

DE8: 5,5'-Dibromo-2,2'-bipyridine (314 mg, 1 mmol), 1,4-diethynylbenzene (126 mg, 1 mmol), $[Pd(PPh_3)_2Cl_2]$ (18 mg, 0.03 mmol), CuI (10 mg, 0.05 mmol), triphenylphosphine (13 mg, 0.05 mmol), *N*,*N*-dimethylformamide (9 mL) and triethylamine (9 mL) were used in this polycondensation reaction described in the general procedure. After work-up and Soxhlet the product was obtained as a yellow solid (268.8 mg, 97%). Anal. Calcd for $(C_{20}H_{10}N_2)_n$: C, 86.31; H, 3.62; N, 10.07%; Found C, 71.54; H, 3.18; N, 8.43%. Pd content: 0.58%, Cu content: 0.64%.

DE9: 2,7-Dibromofluorene (324 mg, 1 mmol), 1,4-diethynylbenzene (126 mg, 1 mmol), $[Pd(PPh_3)_2Cl_2]$ (18 mg, 0.03 mmol), CuI (10 mg, 0.05 mmol), triphenylphosphine (13 mg, 0.05 mmol), *N*,*N*-dimethylformamide (9 mL) and triethylamine (9 mL) were used in this polycondensation reaction described in the general procedure. After work-up and Soxhlet the product was obtained as a yellow solid (185.0 mg, 64%). Anal. Calcd for $(C_{23}H_{12})_n$: C, 95.81; H, 4.19%; Found C, 82.23; H, 3.81%. Pd content: 0.46%, Cu content: 0.07%.

DE10: 3,7-Dibromodibenzo[*b*,*d*]thiophene (342 mg, 1 mmol), 1,4-diethynylbenzene (126 mg, 1 mmol), $[Pd(PPh_3)_2Cl_2]$ (18 mg, 0.03 mmol), CuI (10 mg, 0.05 mmol), triphenylphosphine (13 mg, 0.05 mmol), *N*,*N*-dimethylformamide (9 mL) and triethylamine (9 mL) were used in this polycondensation reaction described in the general procedure. After work-up and Soxhlet the product was obtained as a yellow solid (299.0 mg, 98%). Anal. Calcd for $(C_{22}H_{10}S)_n$: C,

86.25; H, 3.29; S, 10.46%; Found C, 73.50; H, 3.00; S, 9.00%. Pd content: 0.50%, Cu content: 0.06%.

DE11: 3,7-Dibromodibenzo[*b*,*d*]thiophene sulfone (374 mg, 1 mmol), 1,4-diethynylbenzene (126 mg, 1 mmol), [$Pd(PPh_3)_2Cl_2$] (18 mg, 0.03 mmol), CuI (10 mg, 0.05 mmol), triphenylphosphine (13 mg, 0.05 mmol), *N*,*N*-dimethylformamide (9 mL) and triethylamine (9 mL) were used in this polycondensation reaction described in the general procedure. After work-up and Soxhlet the product was obtained as a yellow solid (306.6 mg, 91%). Anal. Calcd for $(C_{22}H_{10}O_2S)_n$: C, 78.09; H, 2.98; S, 9.47%; Found C, 70.00; H, 3.00; S, 9.00%. Pd content: 0.61%, Cu content: 0.04%.

DE12: 2,7-Dibromo-9*H*-carbazole (325 mg, 1 mmol), 1,4-diethynylbenzene (126 mg, 1 mmol), [$Pd(PPh_3)_2Cl_2$] (18 mg, 0.03 mmol), CuI (10 mg, 0.05 mmol), triphenylphosphine (13 mg, 0.05 mmol), *N*,*N*-dimethylformamide (9 mL) and triethylamine (9 mL) were used in this polycondensation reaction described in the general procedure. After work-up and Soxhlet the product was obtained as a yellow solid (139.1 mg, 48%). Anal. Calcd for $(C_{22}H_{11}N)_n$: C, 91.33; H, 3.83; N, 4.84%; Found C, 77.16; H, 3.58; N, 3.61%. Pd content: 0.43%, Cu content: 0.29%.

TEB11: 3,7-Dibromodibenzo[*b*,*d*]thiophene sulfone (374 mg, 1 mmol), 1,3,5-tris(4-ethynyl-phenyl) benzene (252 mg, 0.68 mmol), [$Pd(PPh_3)_2Cl_2$] (18 mg, 0.03 mmol), CuI (10 mg, 0.05 mmol), triphenylphosphine (13 mg, 0.05 mmol), *N*,*N*-dimethylformamide (9 mL) and triethylamine (9 mL) were used in this polycondensation reaction described in the general procedure. After work-up and Soxhlet the product was obtained as a yellow solid (392.7 mg, 73%). Anal. Calcd for $(C_{38}H_{20}O_2S)_n$: C, 84.42; H, 3.73; S, 5.93%; Found C, 75.50; H, 4.00; S, 6.50%. Pd content: 0.48%, Cu content: 0.05%.

TEBN11: 3,7-Dibromodibenzo[*b*,*d*]thiophene sulfone (374 mg, 1 mmol), 2,4,6-tris(4-ethynyl)phenyl]-1,3,5-triazine (254 mg, 0.68 mmol), [$Pd(PPh_3)_2Cl_2$] (18 mg, 0.03 mmol), CuI (10 mg, 0.05 mmol), triphenylphosphine (13 mg, 0.05 mmol), *N*,*N*-dimethylformamide (9 mL) and triethylamine (9 mL) were used in this polycondensation reaction described in the general procedure. After work-up and Soxhlet the product was obtained as a yellow solid (353.0 mg, 65%). Anal. Calcd for $(C_{22}H_{10}O_2N_3S)_n$: C, 77.33; H, 3.15; N, 7.73; S, 5.90%; Found C, 70.50; H, 3.00; N, 5.00; S, 6.50%. Pd content: 0.54%, Cu content: 0.12%.

2 Supporting Figures

2.1 Fourier-transform infrared spectroscopy

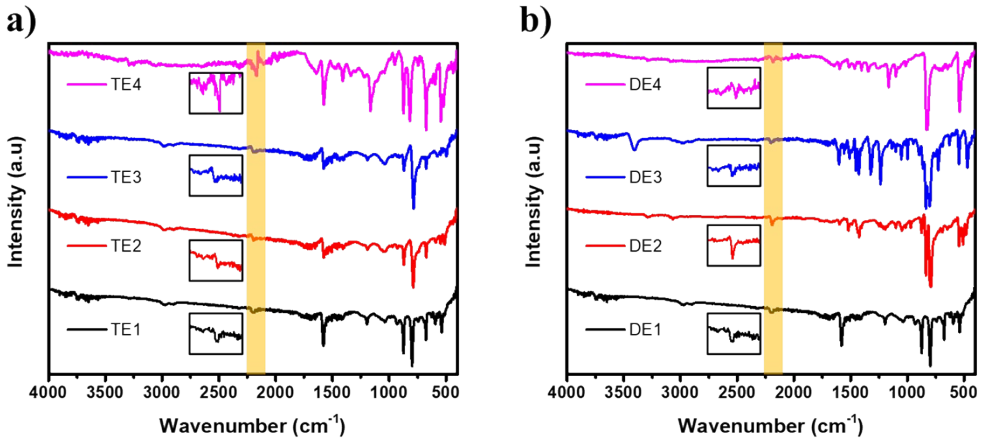

Figure S1: Fourier-transform infrared spectroscopy of TE1-4 and DE1-4.

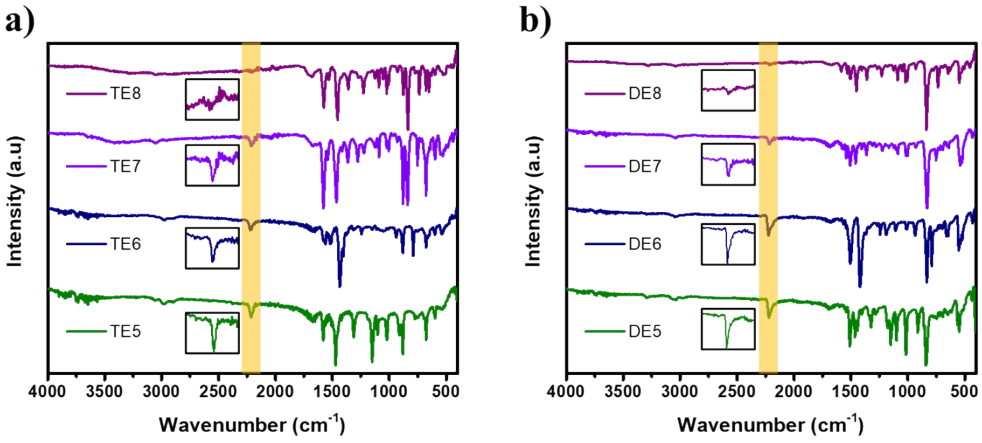

Figure S2: Fourier-transform infrared spectroscopy of TE5-8 and DE5-8.

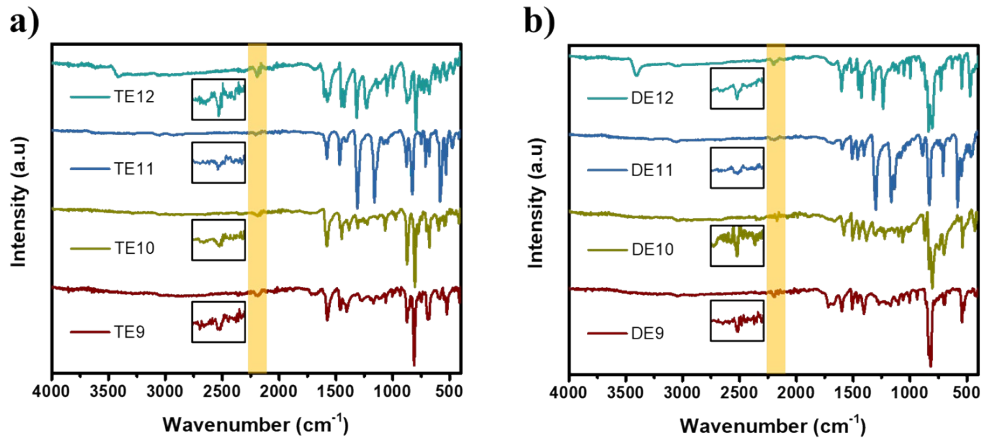

Figure S3: Fourier-transform infrared spectroscopy of TE9-12 and DE9-12.

2.2 Powder X-Ray Diffraction

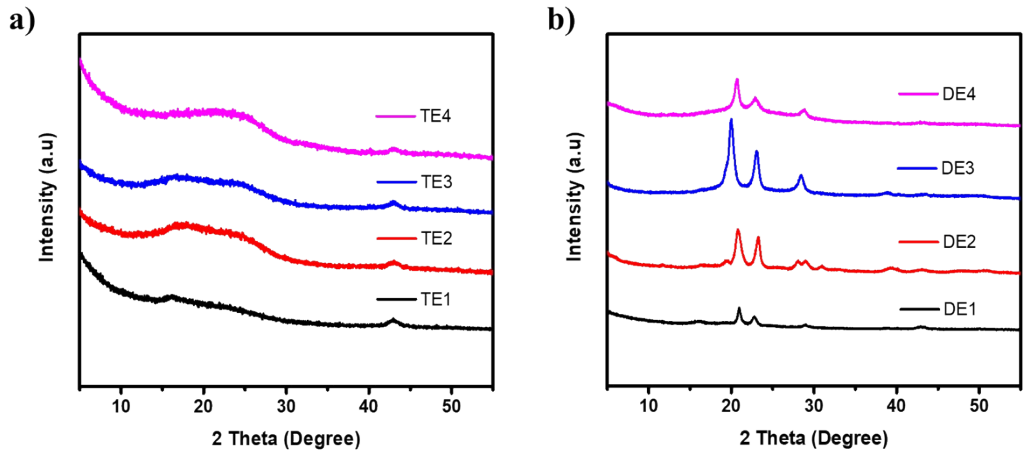

Figure S4: PXRD patterns of a) TE1-4 and b) DE1-4.

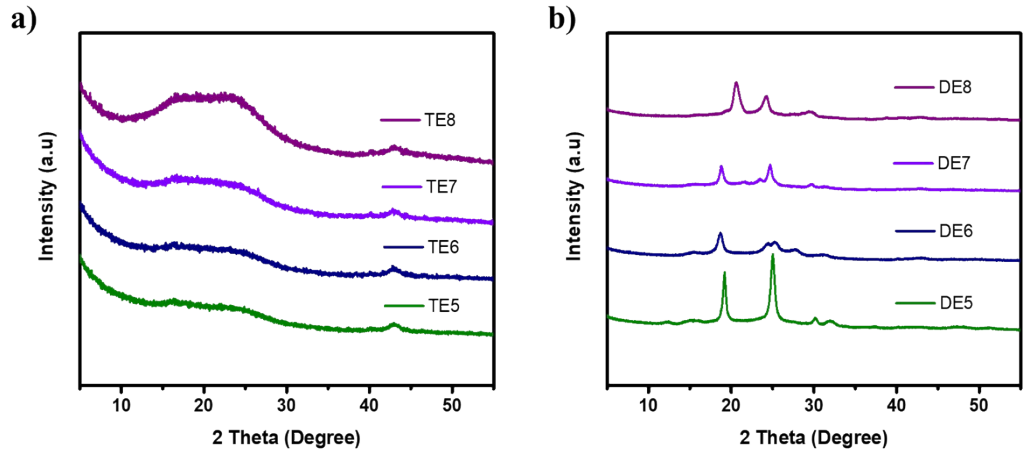

Figure S5: PXRD patterns of a) TE5-8 and b) DE5-8.

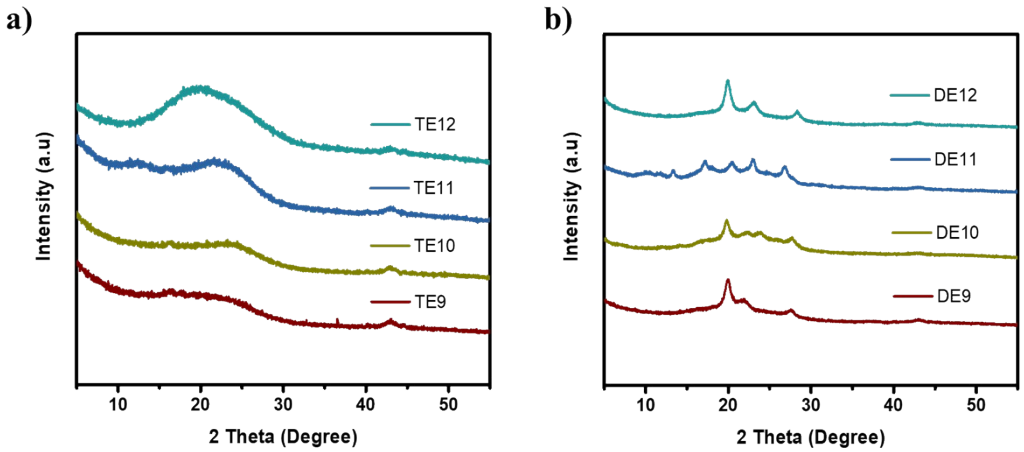

Figure S6: PXRD patterns of TE9-12 and DE9-12.

2.3 Scanning Electron Microscopy

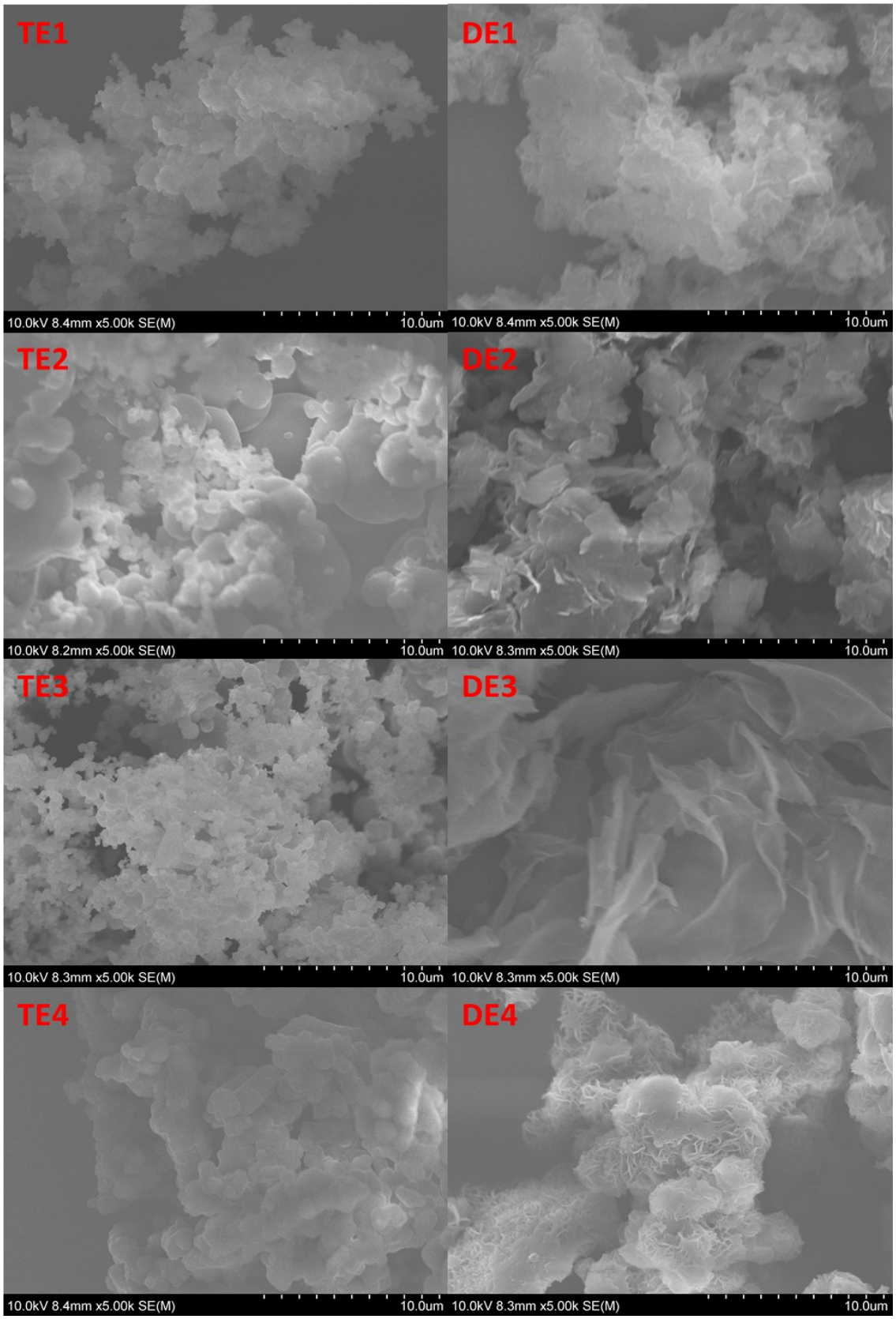

Figure S7: SEM images of TE1-4 and DE1-4.

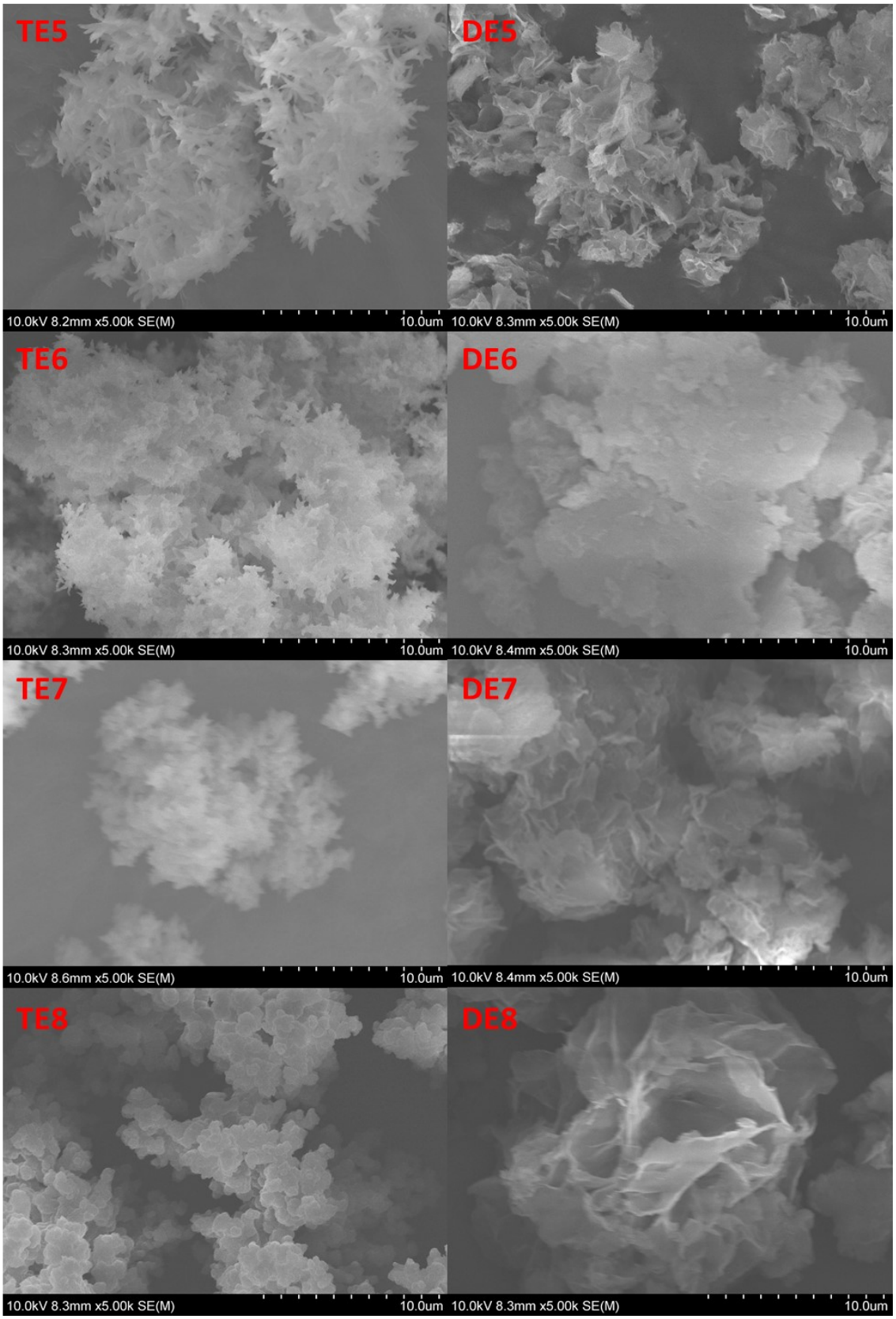

Figure S8: SEM images of TE5-8 and DE5-8.

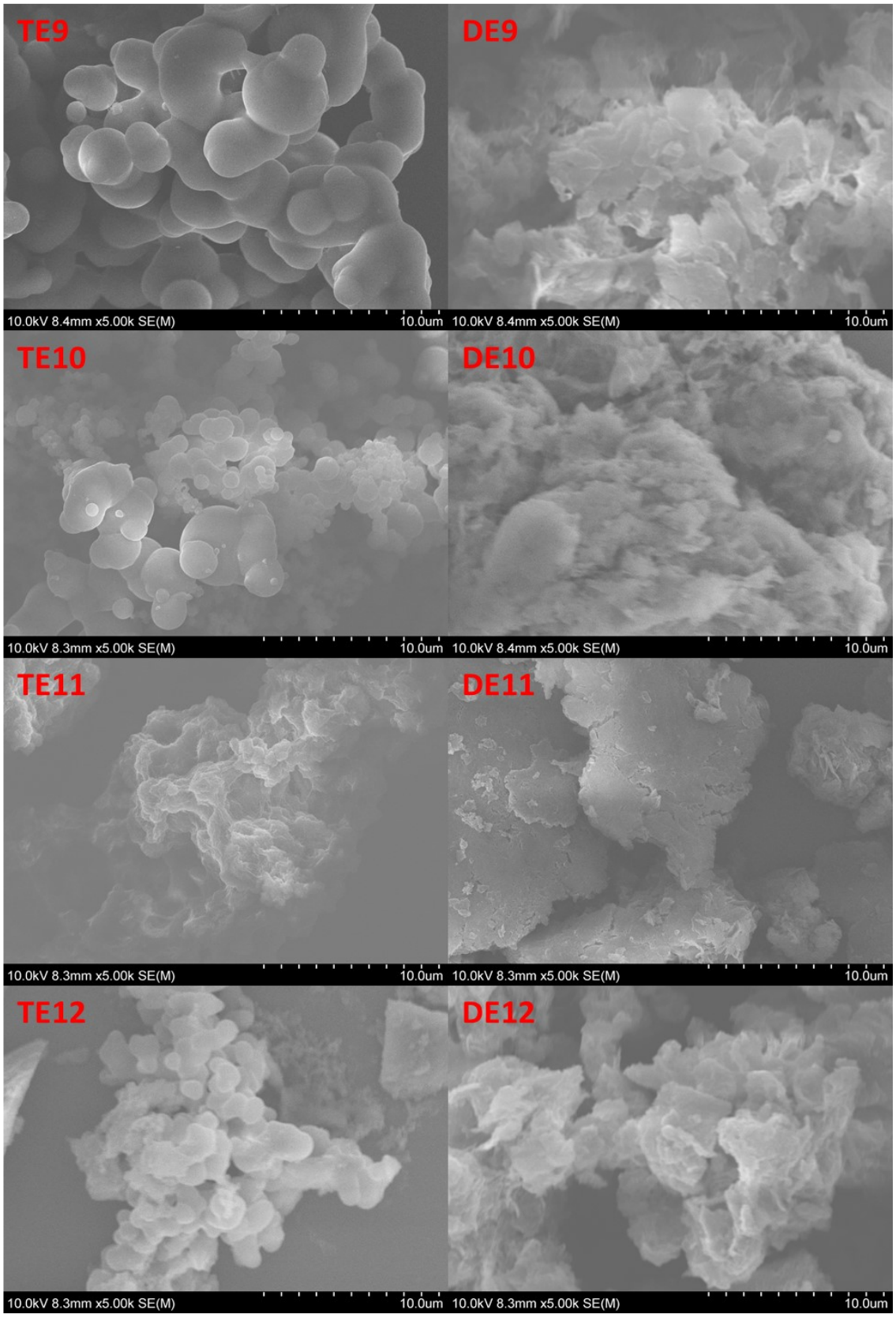

Figure S9: SEM images of TE9-12 and DE9-12.

2.4 Thermogravimetric analysis

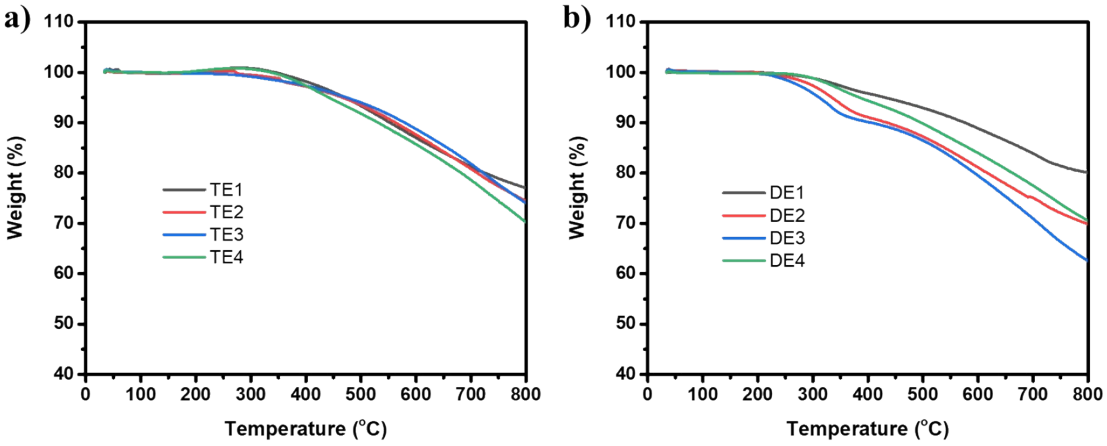

Figure S10: Thermogravimetric data of TE1-4 and DE1-4.

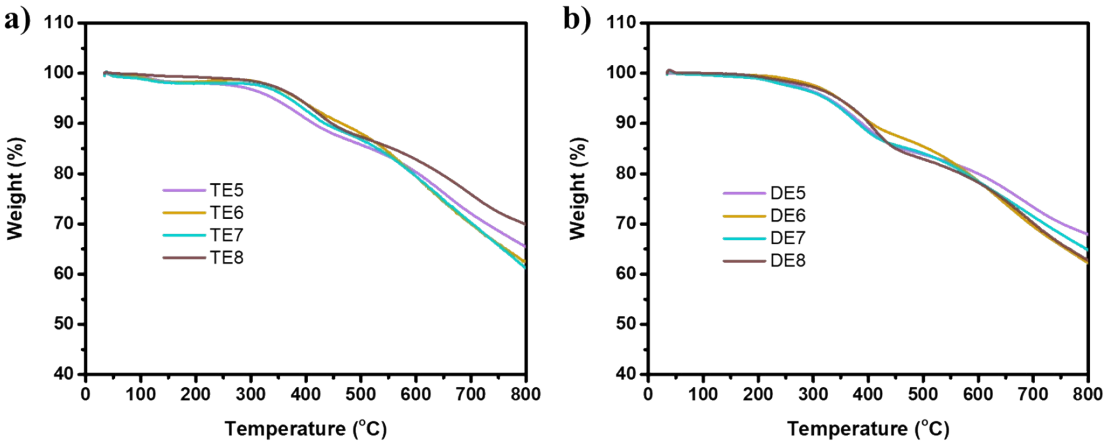

Figure S11: Thermogravimetric data of TE5-8 and DE5-8.

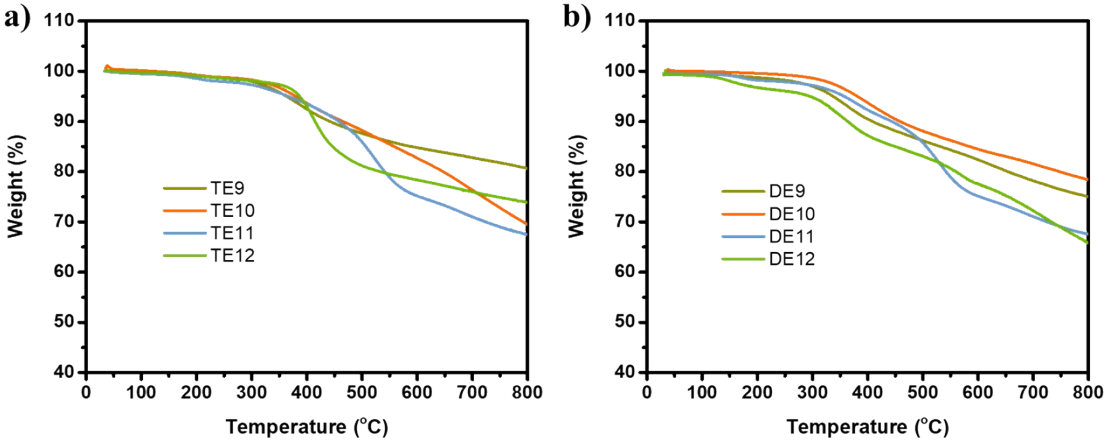

Figure S12: Thermogravimetric data of TE9-12 and DE9-12.

2.5 N_2 Sorption isotherms and Brunauer-Emmett-Teller surface areas

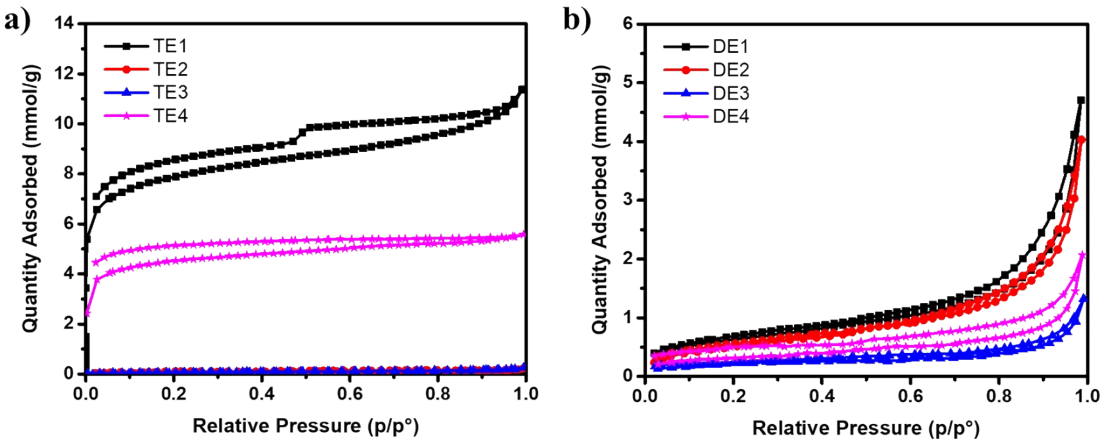

Figure S13: Nitrogen sorption isotherm of TE1-4 and DE1-4.

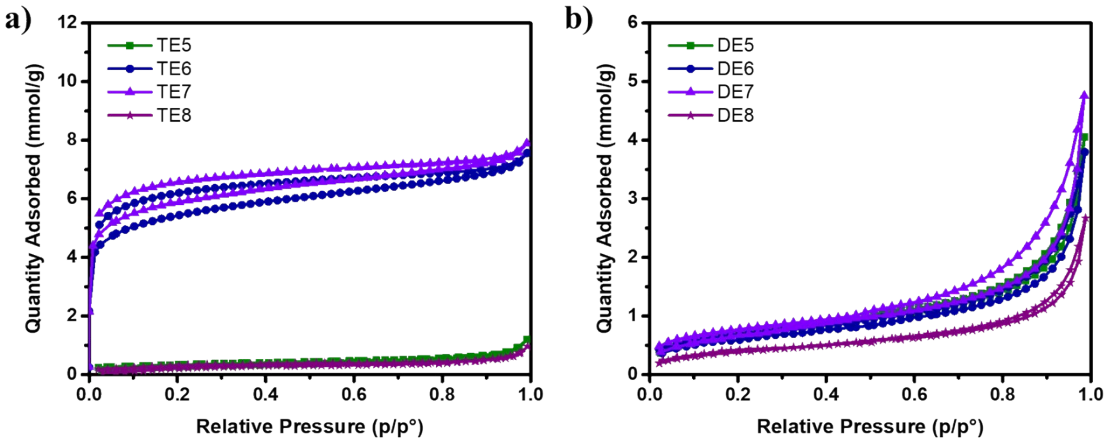

Figure S14: Nitrogen sorption isotherm of TE5-8 and DE5-8.

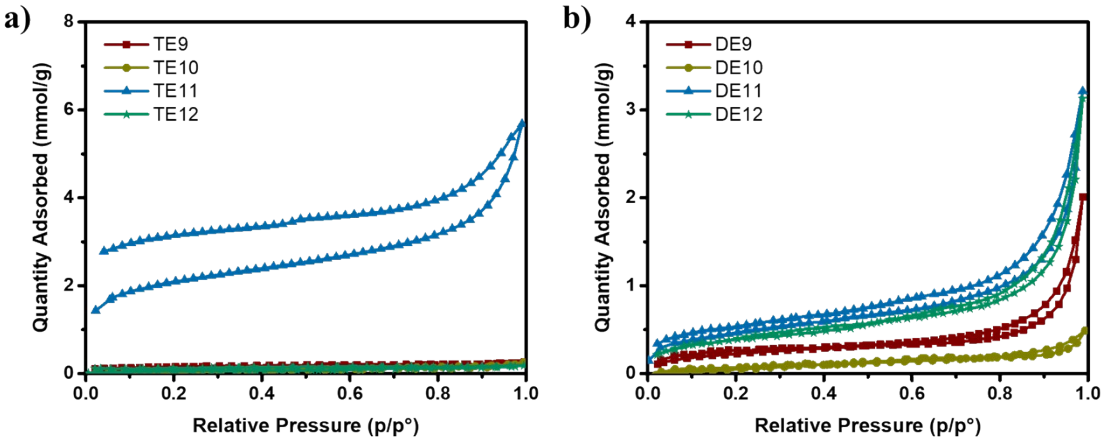

Figure S15: Nitrogen sorption isotherm of TE9-12 and DE9-12.

Table S1: Brunauer-Emmett-Teller surface areas of TE1-12 and DE1-12.

TE-n Polymer	Surface area[a] / $m^2\ g^{-1}$	DE-n Polymer	Surface area[a] / $m^2\ g^{-1}$
TE1	550	DE1	51
TE2	3	DE2	46
TE3	6	DE3	17
TE4	311	DE4	25
TE5	22	DE5	56
TE6	388	DE6	48
TE7	424	DE7	54
TE8	19	DE8	29
TE9	7	DE9	19
TE10	3	DE10	7
TE11	155	DE11	38
TE12	4	DE12	34

[a] BET Surface area determined from the absorption branch of the absorption isotherm measured at 77 K.

2.6 Solid-state UV-visible Spectra

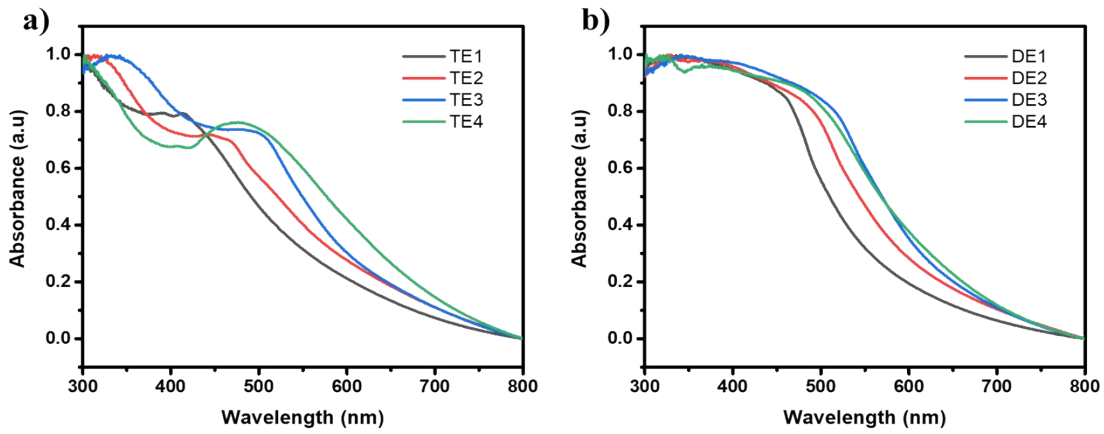

Figure S16: Reflectance UV-visible spectra of TE1-4 and DE1-4 measured in the solid-state.

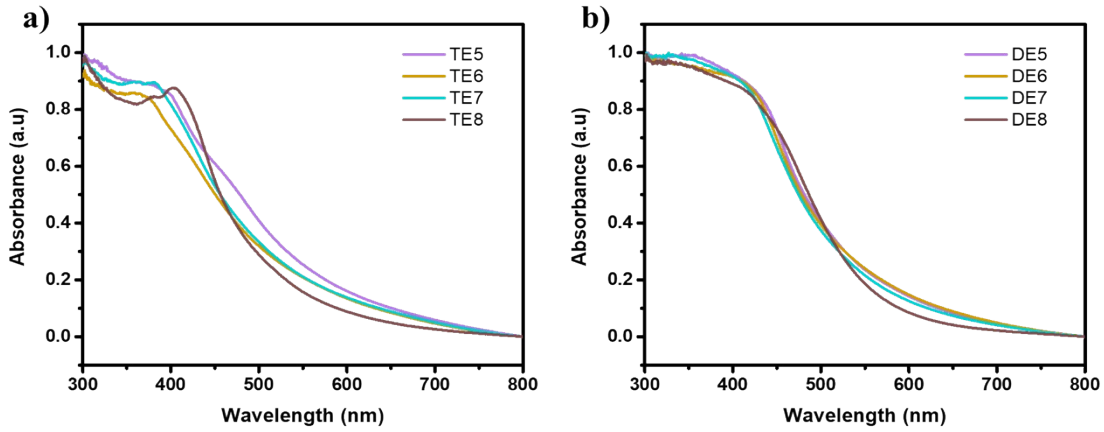

Figure S17: Reflectance UV-visible spectra of TE5-8 and DE5-8 measured in the solid-state.

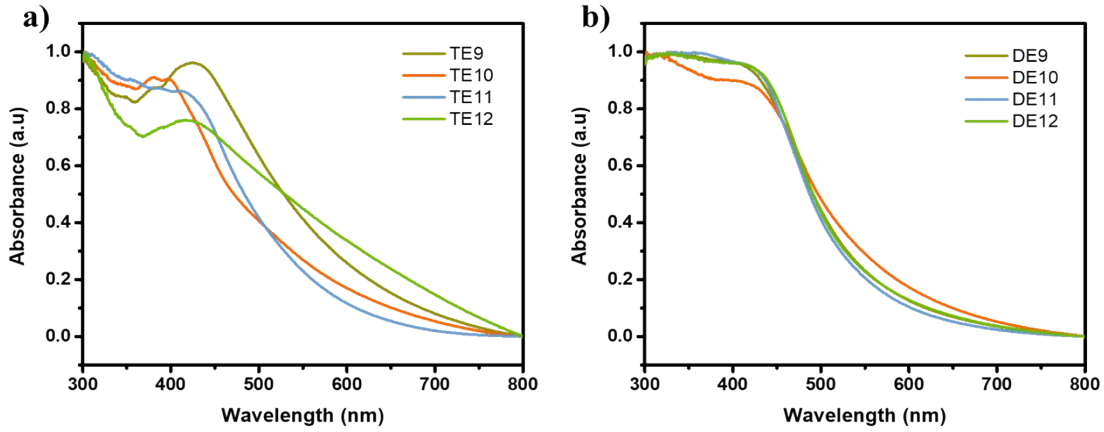

Figure S18: Reflectance UV-visible spectra of TE9-12 and DE9-12 measured in the solid-state.

Table S2: Experimental optical gaps of TE1-12 and DE1-12.

TE-n polymer	$\lambda_{on\text{-}set}$ /nm	Optical gap[a] /eV	Optical gap[b] /eV	DE-n polymer	$\lambda_{on\text{-}set}$ /nm	Optical gap[a] /eV	Optical gap[b] /eV
TE1	644	1.93	2.06	**DE1**	588	2.11	2.24
TE2	685	1.81	1.94	**DE2**	643	1.93	2.07
TE3	695	1.78	1.92	**DE3**	683	1.82	1.95
TE4	750	1.65	1.85	**DE4**	691	1.79	1.93
TE5	623	1.99	2.43	**DE5**	567	2.19	2.37
TE6	588	2.11	2.38	**DE6**	555	2.23	2.42
TE7	572	2.17	2.44	**DE7**	552	2.25	2.44
TE8	530	2.34	2.52	**DE8**	582	2.13	2.28
TE9	646	1.92	2.15	**DE9**	577	2.15	2.31
TE10	572	2.17	2.35	**DE10**	614	2.02	2.18
TE11	587	2.11	2.31	**DE11**	562	2.21	2.34
TE12	743	1.67	2.01	**DE12**	565	2.19	2.33

[a] Calculated from the absorption on-set in the UV-vis spectrum; [b] Calculated from Kubelka-Munk formula based on the spectrum of $(\alpha h\nu)^{\wedge 1/2} \propto E_g$.

2.7 Excitation and emission photoluminescence spectra

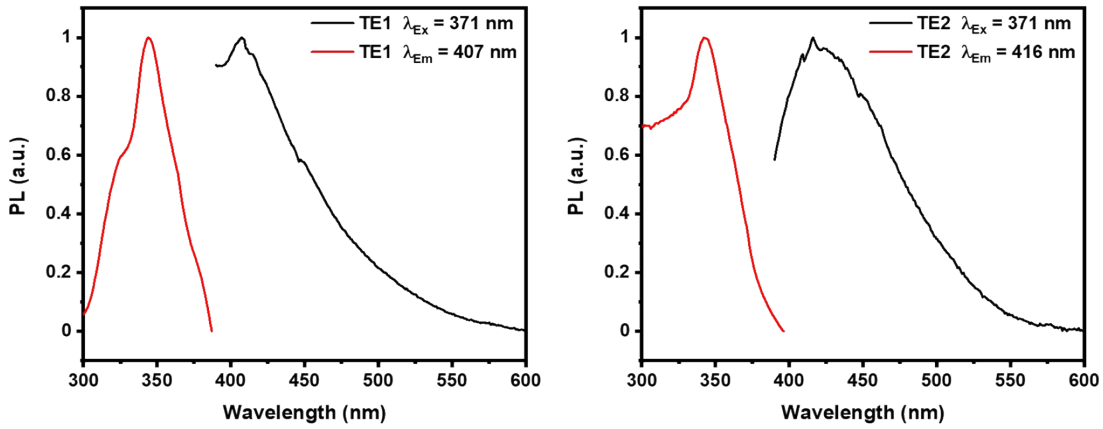

Figure S19: Excitation and emission photoluminescence spectra of TE1 and TE2.

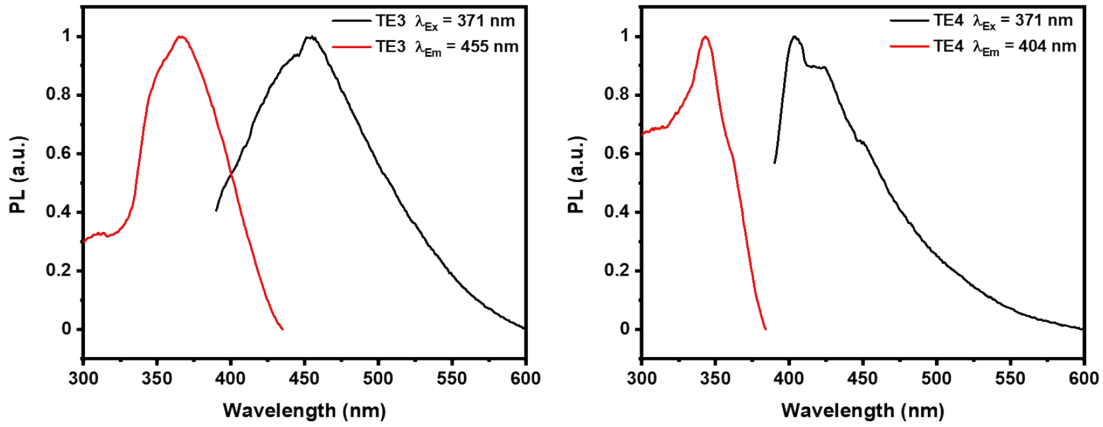

Figure S20: Excitation and emission photoluminescence spectra of TE3 and TE4.

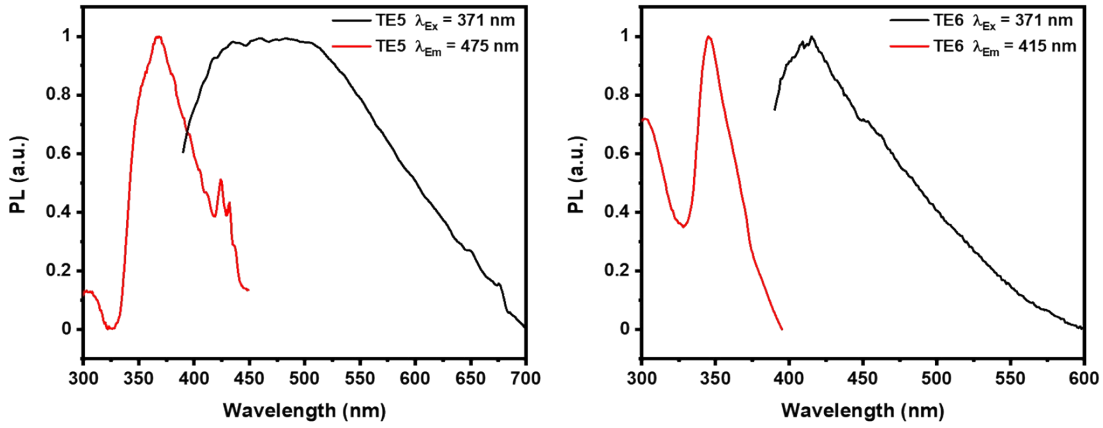

Figure S21: Excitation and emission photoluminescence spectra of TE5 and TE6.

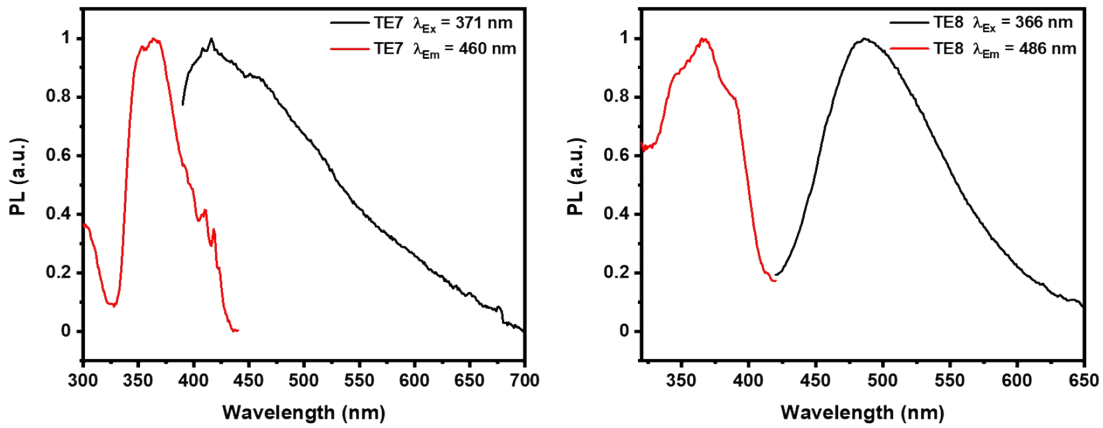

Figure S22: Excitation and emission photoluminescence spectra of TE7 and TE8.

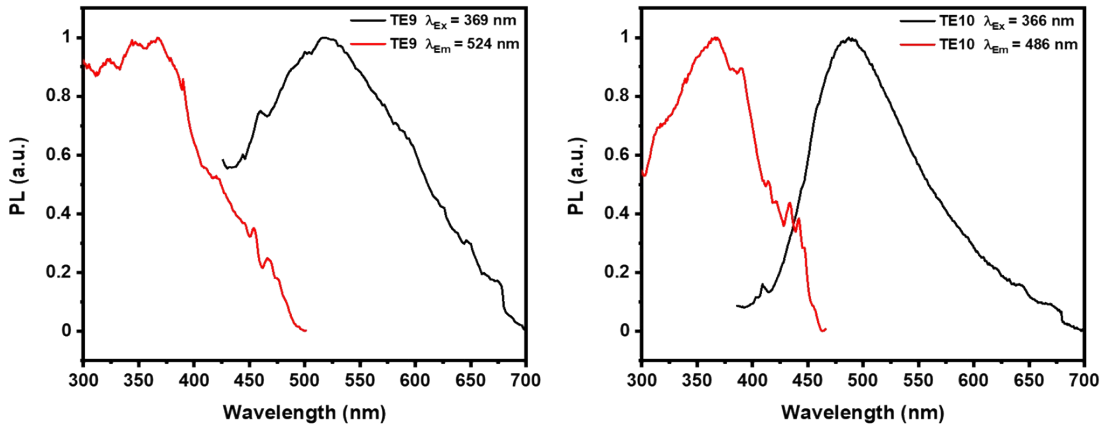

Figure S23: Excitation and emission photoluminescence spectra of TE9 and TE10.

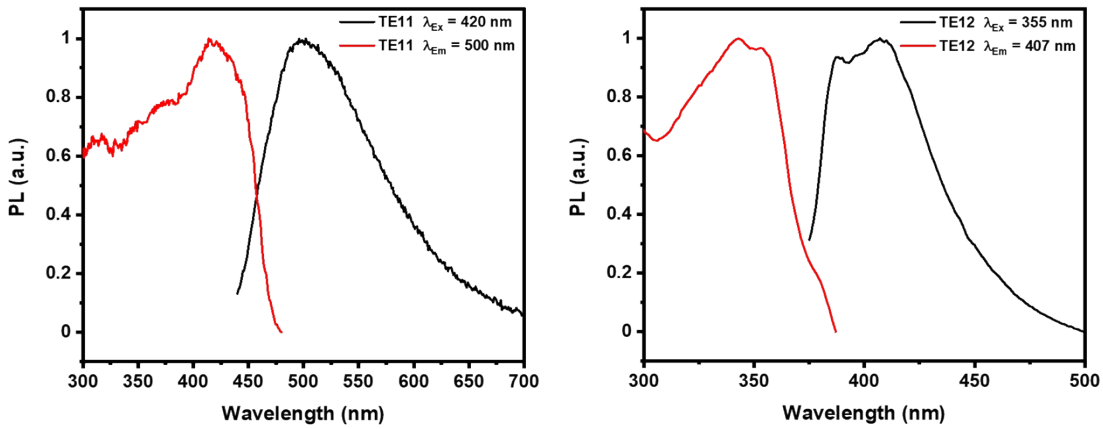

Figure S24: Excitation and emission photoluminescence spectra of TE11 and TE12.

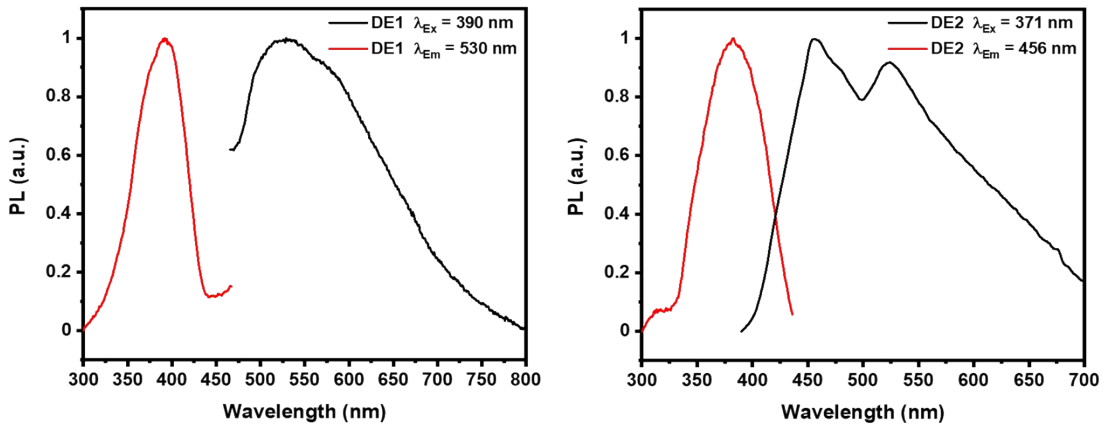

Figure S25: Excitation and emission photoluminescence spectra of DE1 and DE2.

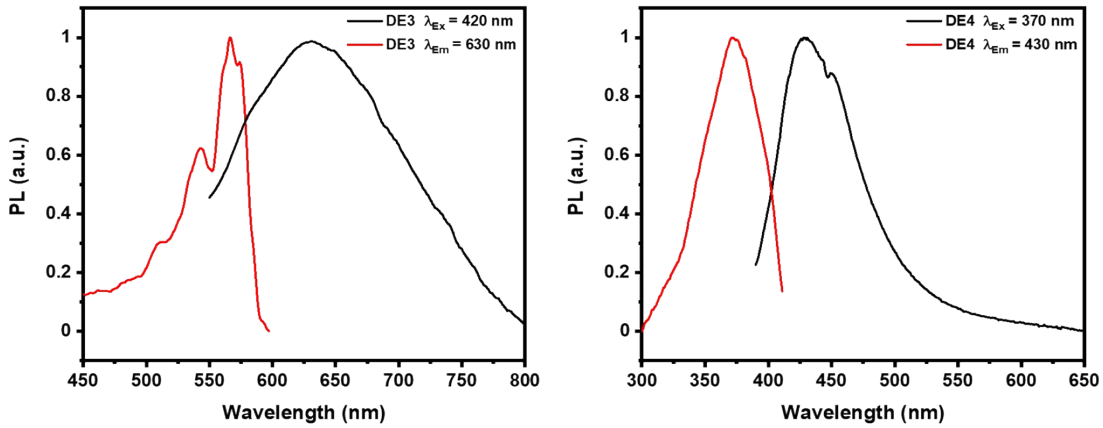

Figure S26: Excitation and emission photoluminescence spectra of DE3 and DE4.

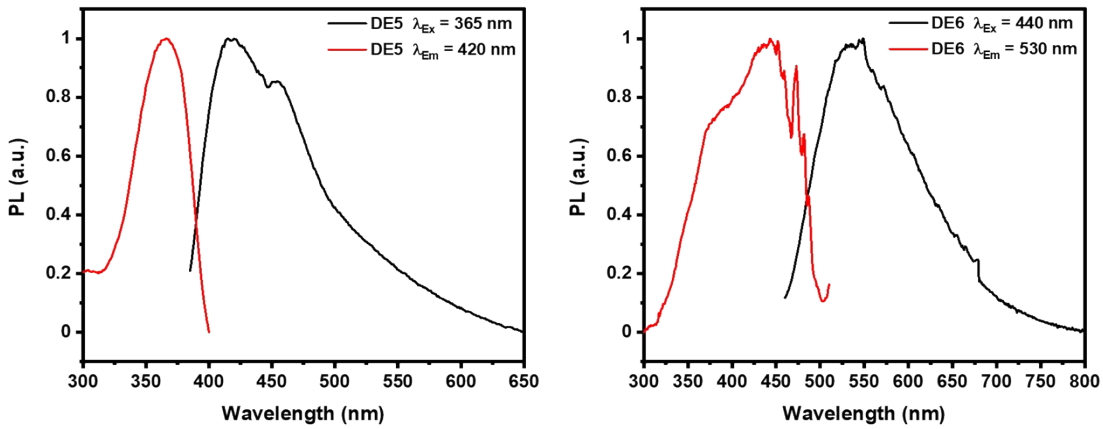

Figure S27: Excitation and emission photoluminescence spectra of DE5 and DE6.

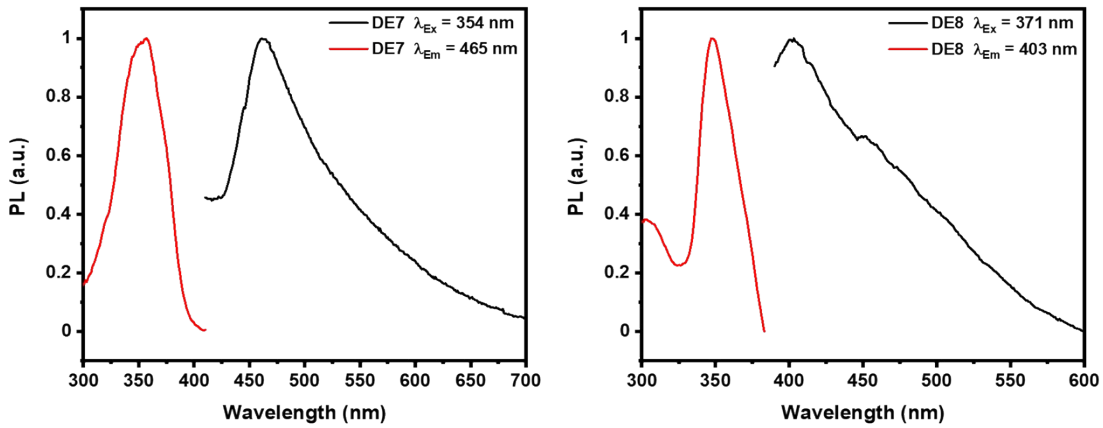

Figure S28: Excitation and emission photoluminescence spectra of DE7 and DE8.

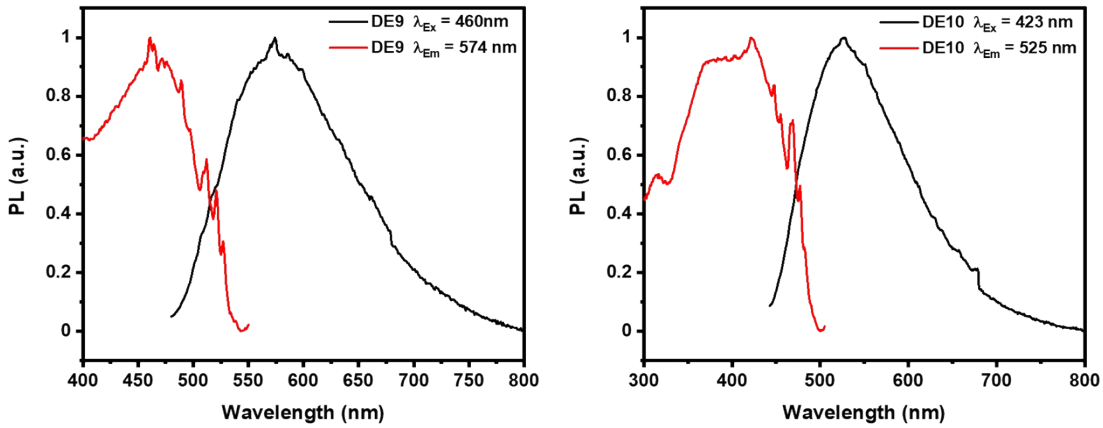

Figure S29: Excitation and emission photoluminescence spectra of DE9 and DE10.

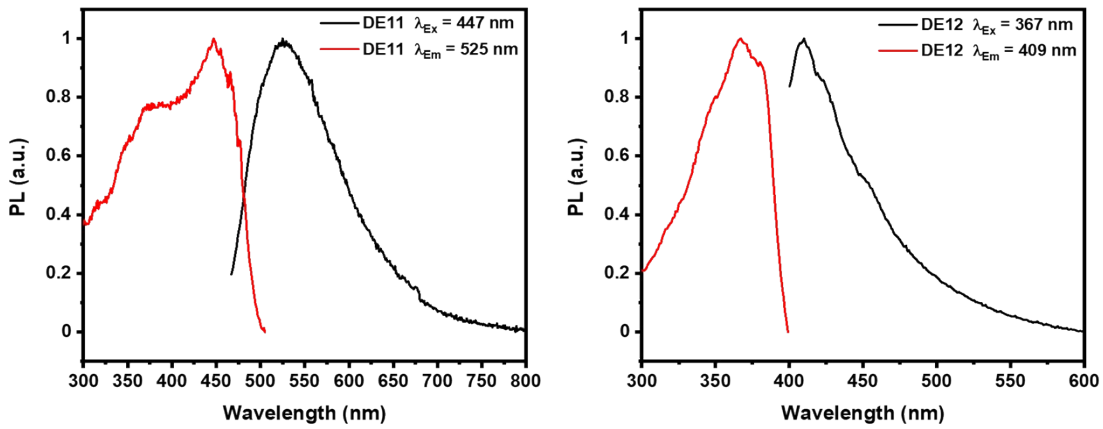

Figure S30: Excitation and emission photoluminescence spectra of DE11 and DE12.

2.8 Time-Correlated Single Photon Counting Experiments

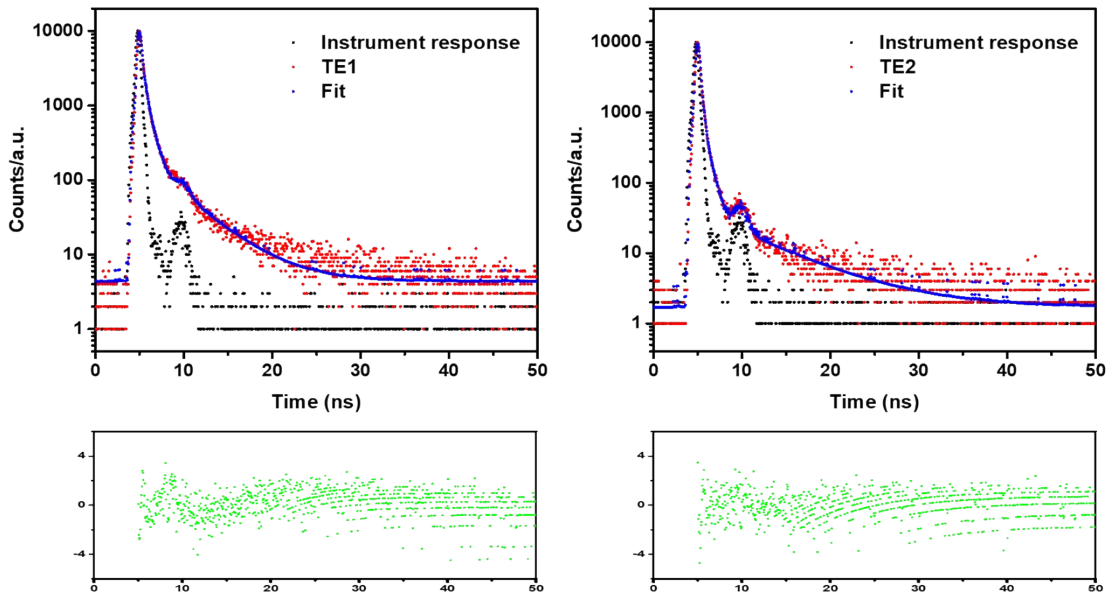

Figure S31: Fluorescence life-time decays of TE1 and TE2.

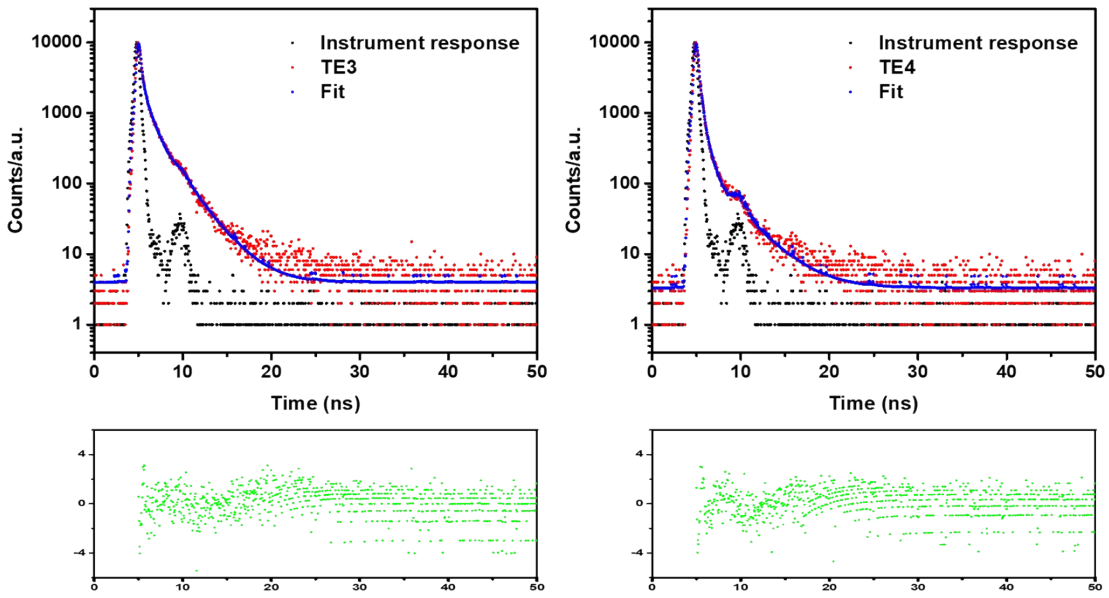

Figure S32: Fluorescence life-time decays of TE3 and TE4.

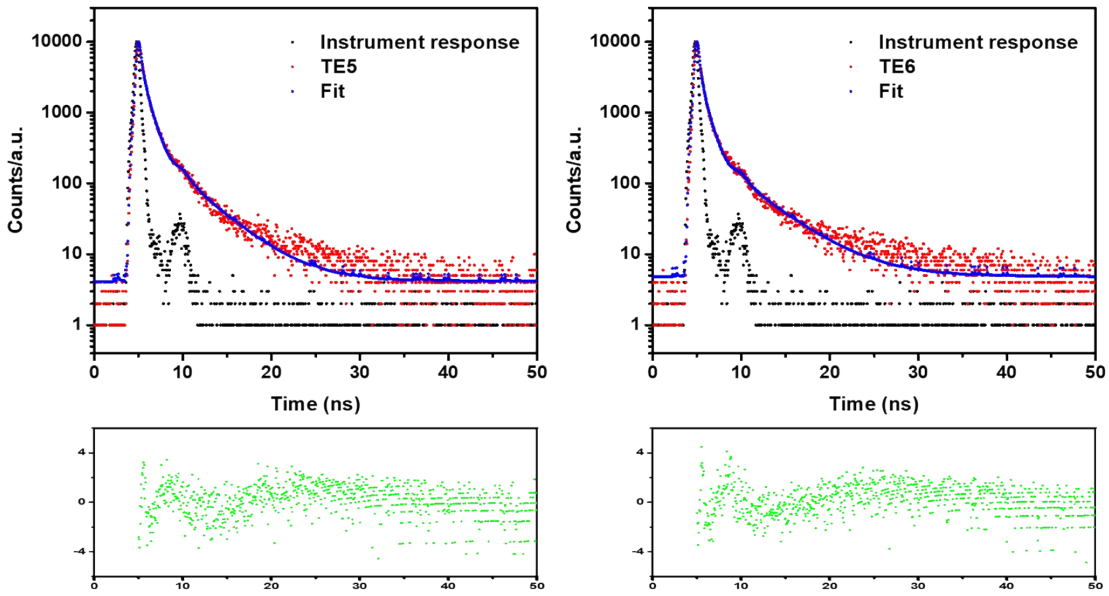

Figure S33: Fluorescence life-time decays of TE5 and TE5.

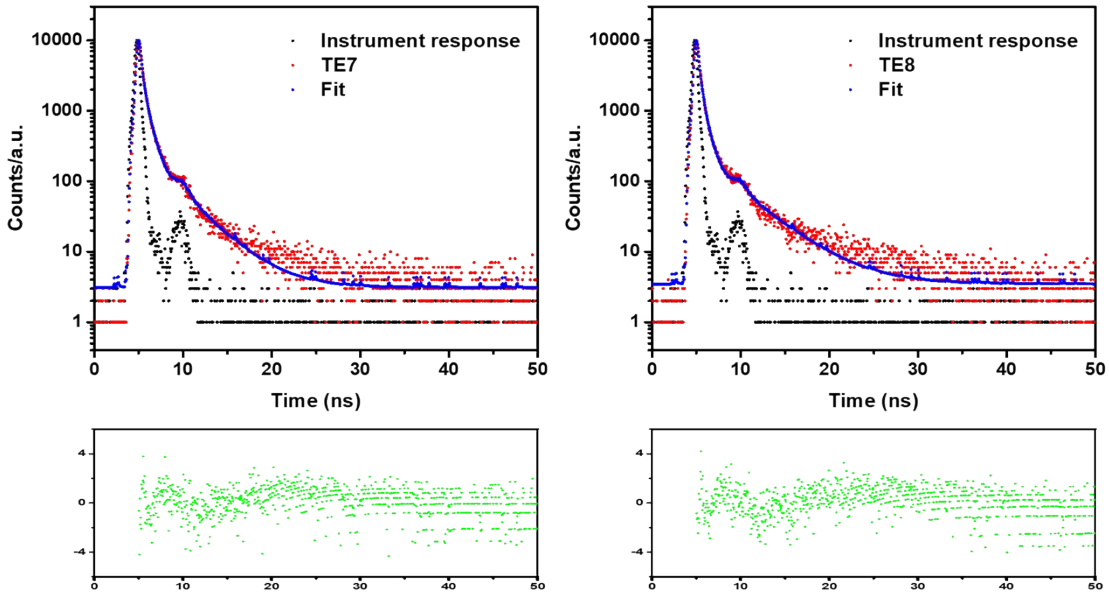

Figure S34: Fluorescence life-time decays of TE7 and TE8.

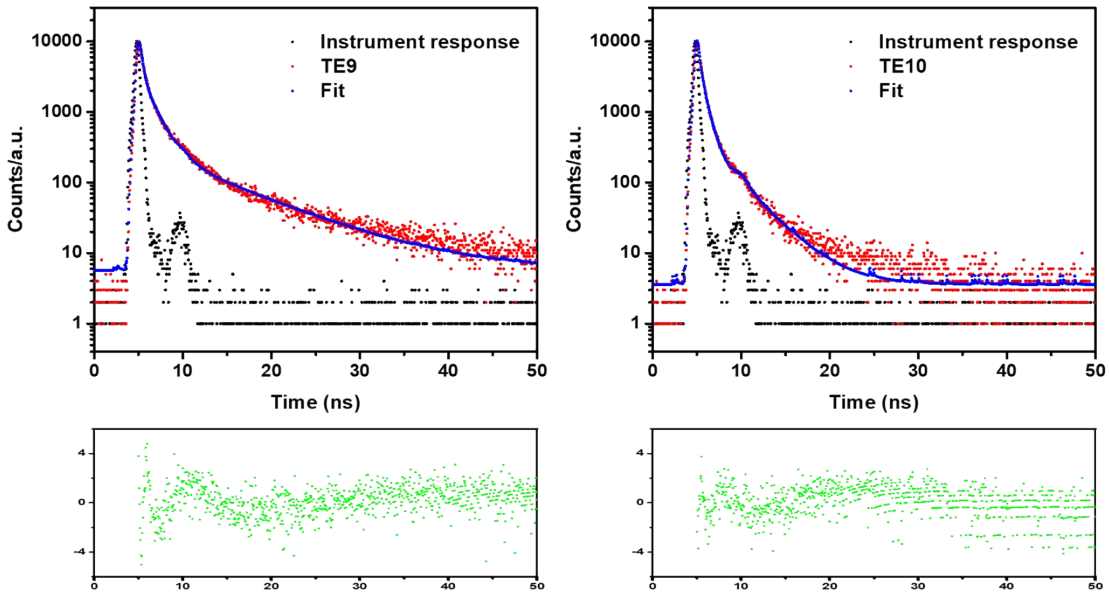

Figure S35: Fluorescence life-time decays of TE9 and TE10.

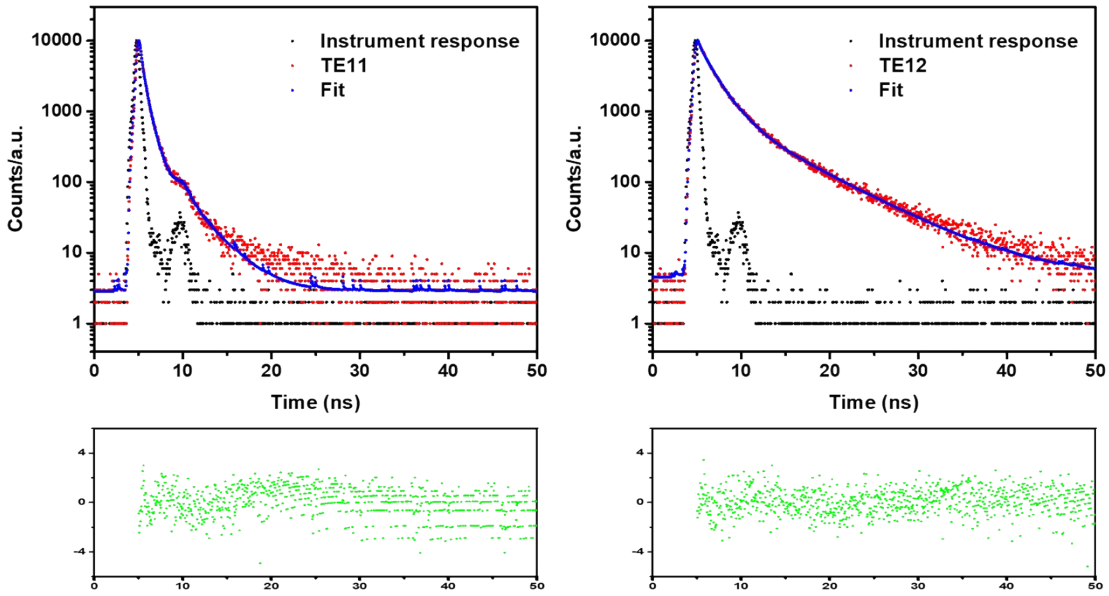

Figure S36: Fluorescence life-time decays of TE11 and TE12.

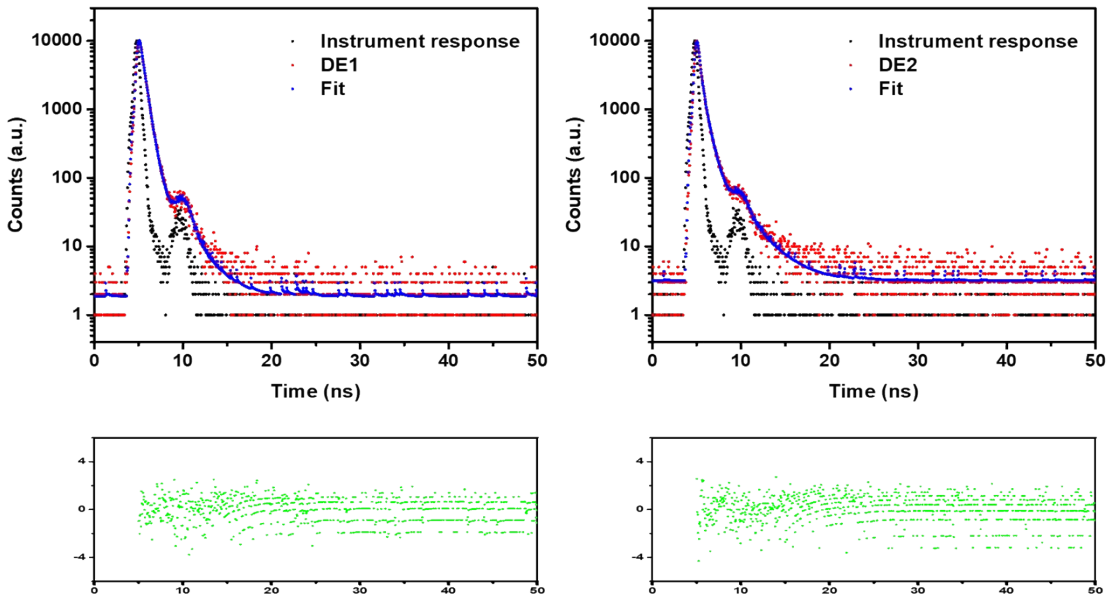

Figure S37: Fluorescence life-time decays of DE1 and DE2.

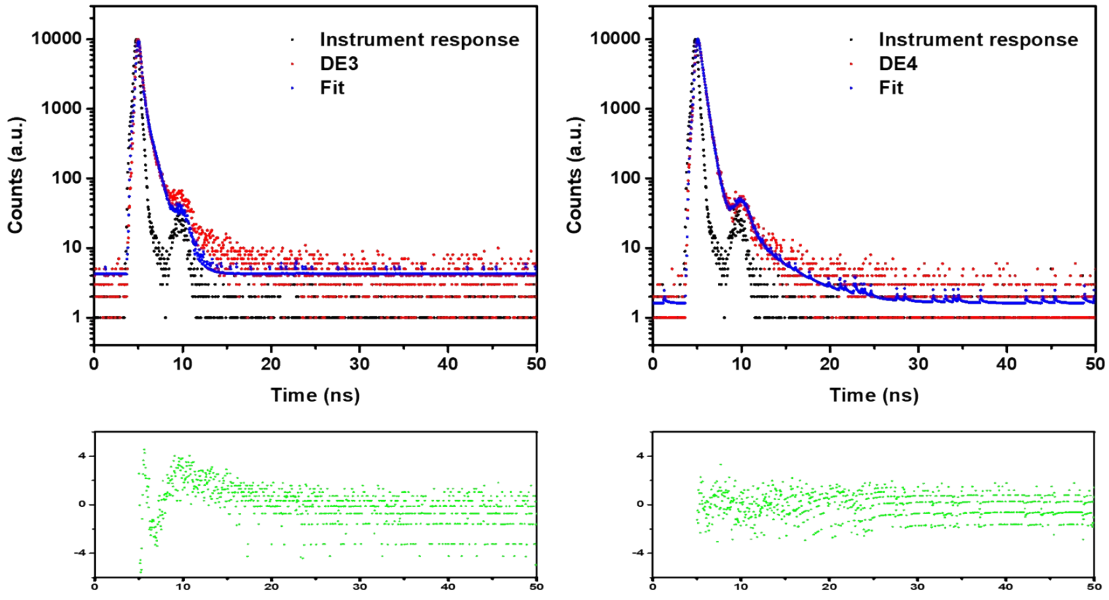

Figure S38: Fluorescence life-time decays of DE3 and DE4.

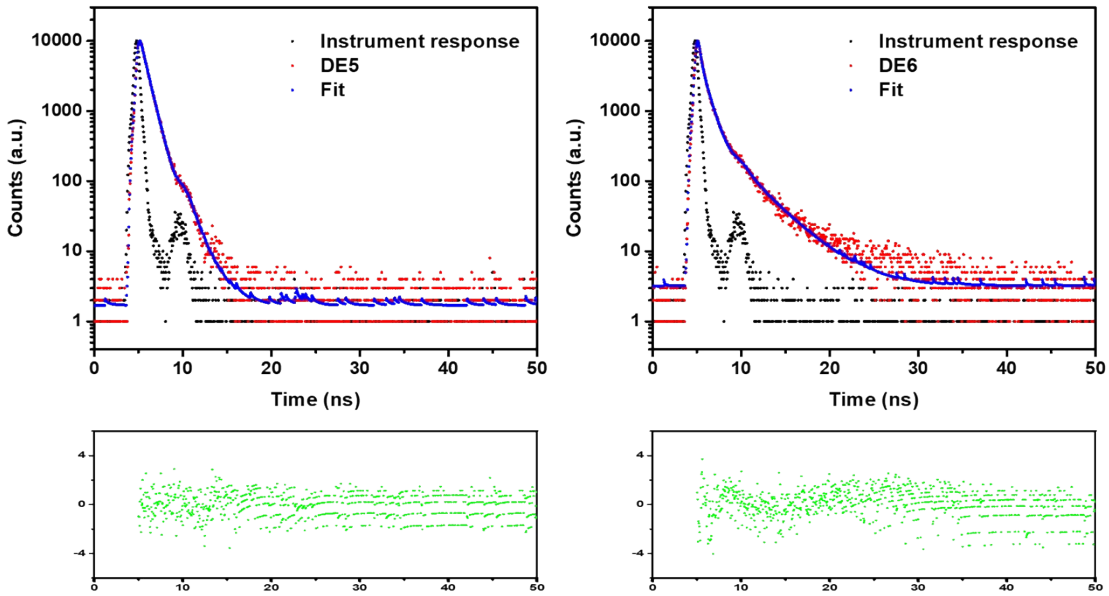

Figure S39: Fluorescence life-time decays of DE5 and DE6.

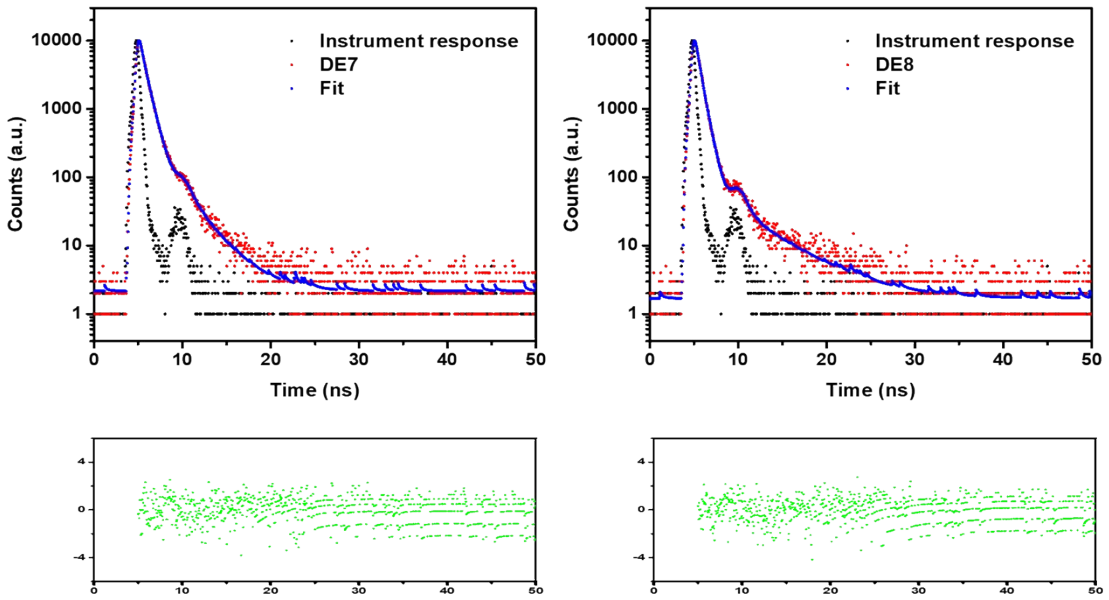

Figure S40: Fluorescence life-time decays of DE7 and DE8.

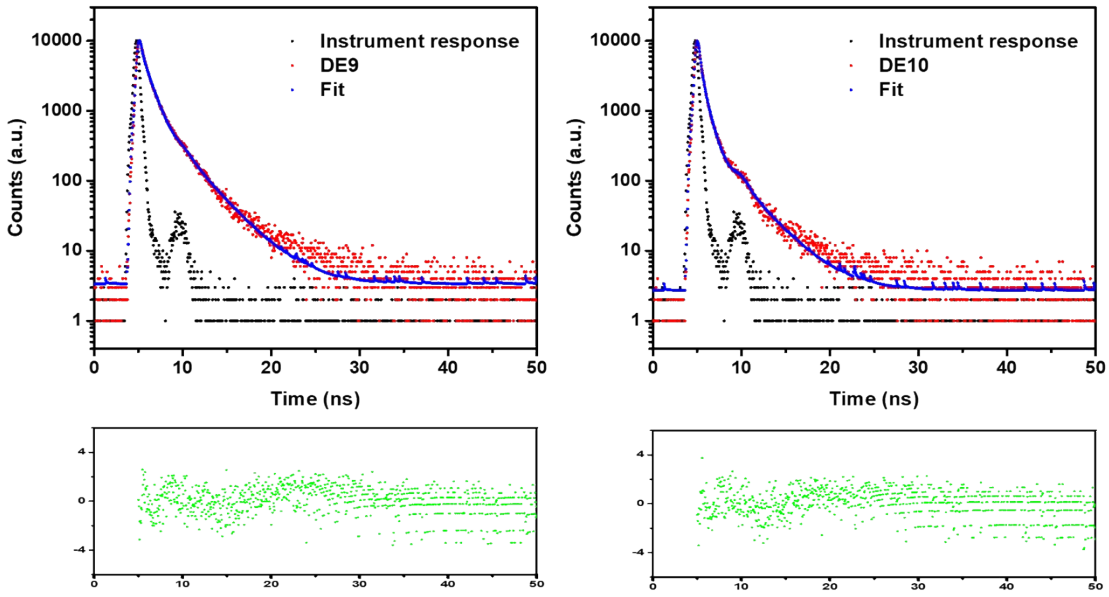

Figure S41: Fluorescence life-time decays of DE9 and DE10.

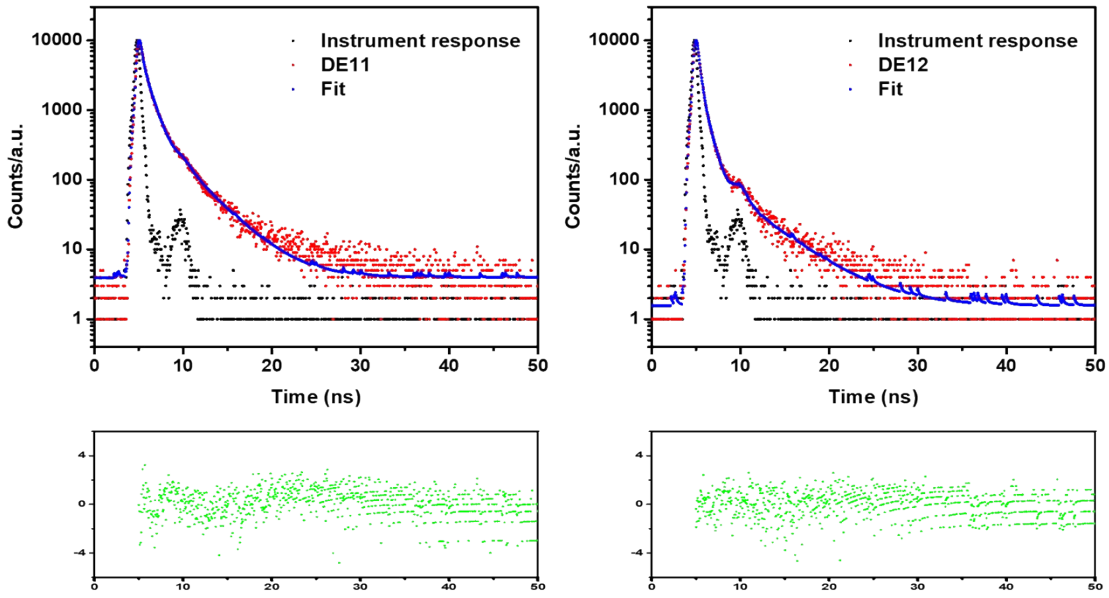

Figure S42: Fluorescence life-time decays of DE11 and DE12.

Table S3: Estimated fluorescence lifetimes of TE1-12 and DE1-12.

Polymer	λ_{em} / nm	τ_1 / ns	B_1 / %	τ_2 / ns	B_2 / %	τ_3 / ns	B_3 / %	χ^2	τ_{avg} / ns
TE1	407	0.15	67.06	0.80	26.53	4.85	6.40	1.443	0.63
TE2	416	0.07	83.95	0.59	13.58	6.28	2.47	1.195	0.29
TE3	455	0.14	59.86	1.05	26.44	2.89	13.70	1.604	0.76
TE4	404	0.08	73.29	0.54	20.90	2.93	5.81	1.495	0.34
TE5	475	0.23	53.51	1.05	37.10	4.98	9.40	1.530	0.98
TE6	415	0.21	61.39	1.04	29.63	5.55	8.98	1.387	0.94
TE7	460	0.16	66.01	0.84	27.53	4.32	6.46	1.475	0.62
TE8	486	0.15	68.48	0.78	23.68	4.86	7.83	1.570	0.67
TE9	524	0.32	49.89	1.47	34.27	7.55	15.84	1.324	1.86
TE10	486	0.20	56.76	0.90	34.46	4.16	8.78	1.577	0.79
TE11	500	0.20	53.21	0.78	40.51	3.68	6.28	1.531	0.66
TE12	407	1.16	46.54	2.32	36.19	7.00	17.27	1.147	2.59
DE1	530	0.16	36.91	0.52	60.86	2.69	2.23	1.128	0.43
DE2	456	0.13	63.56	0.64	32.49	2.91	3.95	1.462	0.41
DE3	630	0.09	73.56	0.58	22.89	2.71	3.55	1.442	0.30
DE4	430	0.20	42.23	0.53	56.32	5.26	1.46	1.090	0.46
DE5	420	0.26	18.65	0.83	79.66	2.83	1.69	1.028	0.76
DE6	530	0.29	45.77	1.06	43.33	4.20	10.90	1.370	1.05
DE7	465	0.26	27.72	0.76	66.86	3.18	5.42	1.228	0.75
DE8	403	0.35	46.72	0.68	50.40	5.85	2.88	1.108	0.67
DE9	574	0.32	30.45	1.20	53.43	3.66	16.13	1.336	1.33
DE10	525	0.18	55.54	0.82	35.27	3.56	9.19	1.369	0.72
DE11	525	0.27	42.07	1.09	45.92	3.97	12.00	1.541	1.09
DE12	409	0.16	60.26	0.72	33.91	4.64	5.84	1.255	0.61

[a] Fluorescence lifetimes for all polymers obtained from fitting time-correlated single photon counting decays to a sum of three exponentials, which yield τ_1, τ_2, and τ_3 according $\sum_{i=1}^{n}(A + B_i exp(-t/\tau_i))$. τ_{avg} is the weighted average lifetime calculated as $\sum_{i=1}^{n}(B_i\tau_i)$.

2.9 Contact angle measurements

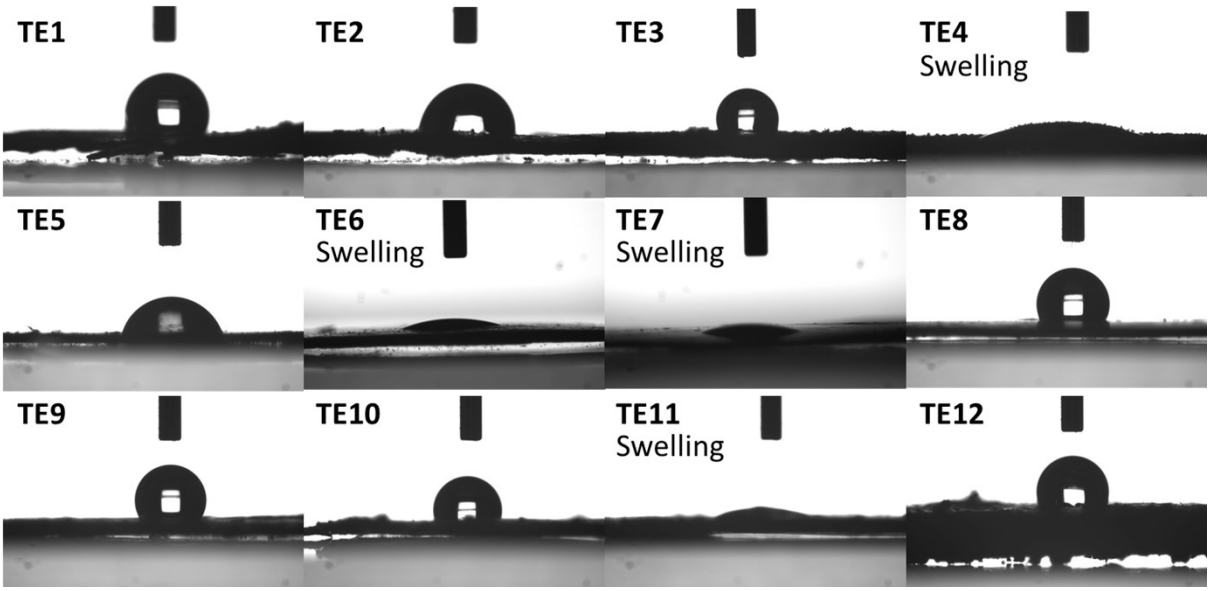

Figure S43: Contact angle images against water of TE1-12. For materials that swell, the image was taken immediately after the water droplet was deposited onto the polymer pallet.

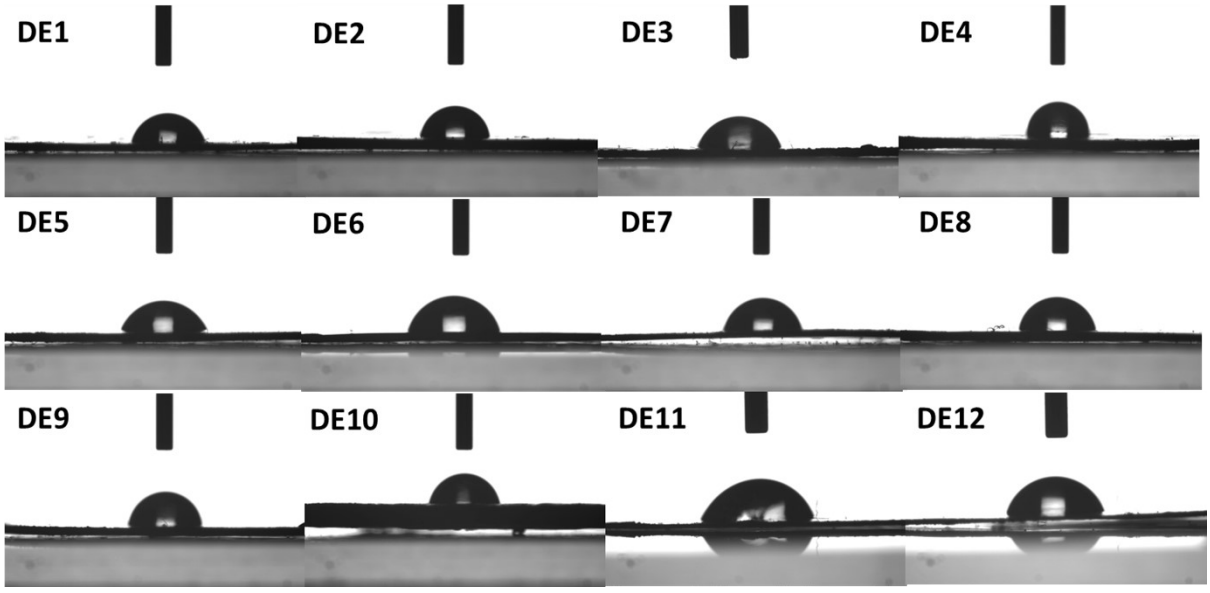

Figure S44: Contact angle images against water of DE1-12.

Table S4: Contact angles against water of TE1-12 and DE1-12 pallets.

TE-n Polymer	Contact angle against water / °	DE-n Polymer	Contact angle against water / °
TE1	100.1 (±2.1)	**DE1**	80.9 (±2.3)
TE2	84.9 (±1.4)	**DE2**	86.9 (±2.1)
TE3	101.9 (±1.1)	**DE3**	76.0 (±0.7)
TE4	Swelling	**DE4**	94.0 (±5.1)
TE5	59.5 (±1.3)	**DE5**	80.2 (±2.1)
TE6	Swelling	**DE6**	75.9 (±2.0)
TE7	Swelling	**DE7**	80.8 (±2.0)
TE8	115.7 (±0.7)	**DE8**	84.9 (±1.8)
TE9	113.3 (±1.8)	**DE9**	87.5 (±0.8)
TE10	104.8 (±0.9)	**DE10**	77.6 (±2.1)
TE11	Swelling	**DE11**	76.7 (±2.7)
TE12	103.7 (±4.4)	**DE12**	84.1 (±2.1)

Table S5: Average transmission values of TE1-12 and DE1-12.

TE-n Polymer	Transmission TEA/MeOH/H_2O / %	DE-n Polymer	Transmission TEA/MeOH/H_2O / %
TE1	5.8	**DE1**	2.3
TE2	50.5	**DE2**	1.7
TE3	71.5	**DE3**	28.3
TE4	40.0	**DE4**	21.7
TE5	0.5	**DE5**	15.0
TE6	4.3	**DE6**	2.4
TE7	4.6	**DE7**	16.3
TE8	12.8	**DE8**	4.6
TE9	71.2	**DE9**	3.3
TE10	12.2	**DE10**	78.8
TE11	28.8	**DE11**	6.6
TE12	84.6	**DE12**	18.9

2.10 Static light scattering

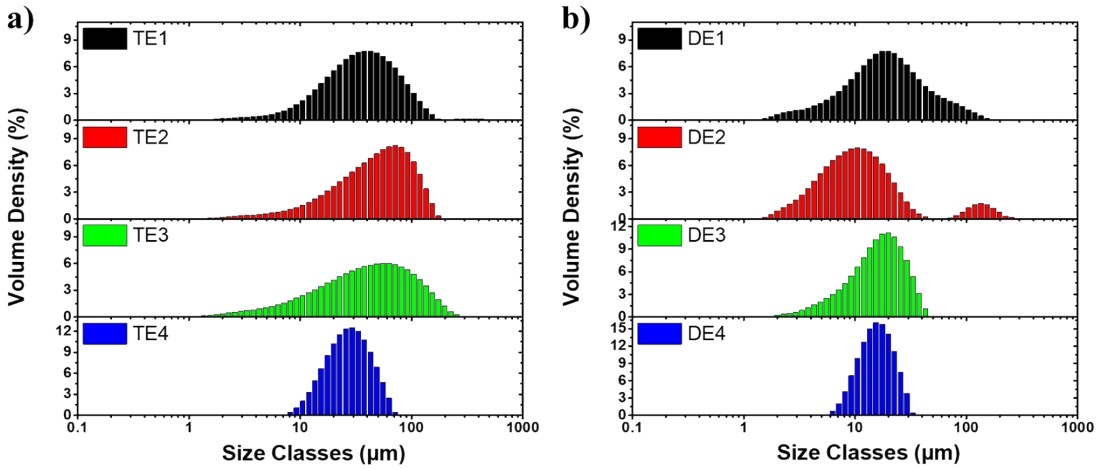

Figure S45: Static light scattering experiments of a) TE1-4 and b) DE1-4.

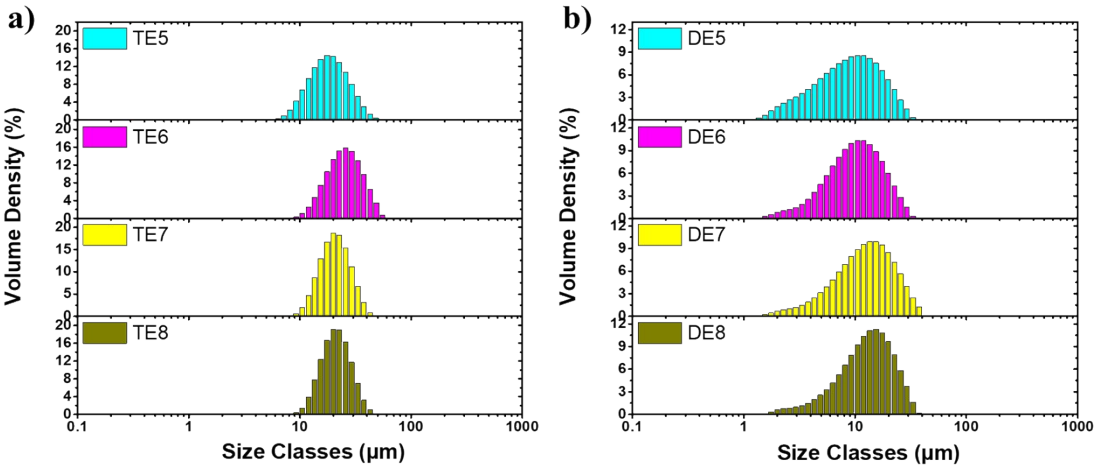

Figure S46: Static light scattering experiments of a) TE5-8and b) DE5-8.

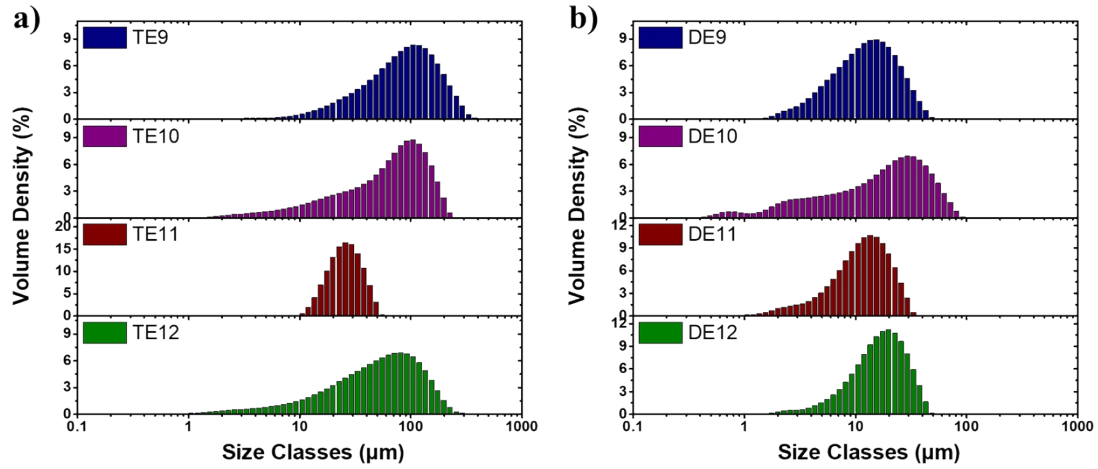

Figure S47: Static light scattering experiments of a) TE9-12 and b) DE9-12.

Table S6: Particle sizes by static light scattering of TE1-12 and DE1-12.

Polymer	*Dx*50[a] / µm	*D*[4,3][b] / µm	*D*[3,2][c] / µm	Relative external surface area[d] / m^2 kg^{-1}
TE1	35.5	45.2	22.5	266.7
TE2	48.8	55.3	25.8	232.9
TE3	40.4	54.0	19.1	314.6
TE4	27.0	29.2	24.0	250.2
TE5	18.1	19.4	16.7	359.1
TE6	25.0	26.3	23.2	258.1
TE7	20.6	21.4	19.6	306.4
TE8	21.0	21.9	20.0	299.3
TE9	86.1	99.1	49.3	121.8
TE10	68.5	74.2	26.1	229.7
TE11	25.5	26.7	23.9	251.5
TE12	51.9	63.4	20.6	290.8
DE1	18.5	25.8	12.1	494.3
DE2	10.3	22.3	8.03	747.6
DE3	16.3	17.3	12.1	496.1
DE4	15.5	16.2	14.4	416.2
DE5	8.9	10.3	6.53	918.8
DE6	10.1	11.2	7.94	755.3
DE7	12.5	13.8	9.27	647.1
DE8	13.1	13.9	9.89	606.7
DE9	12.5	14.3	9.18	653.8
DE10	18.5	22.2	6.44	931.8
DE11	11.7	12.5	8.12	739.1
DE12	16.9	18.0	12.6	475.1

[a] 50^{th} Percentile of particle size volume distribution; [b] Volume mean diameter; [c] Surface area mean diameter (Sauter mean diameter);[1] [d] Relative extrinsic surface area calculated by dividing the total surface area of the particles by the total mass, assuming a density of 1 g cm^{-3}.

2.11 Calculations of EA and IP of TE1-12 and DE1-12

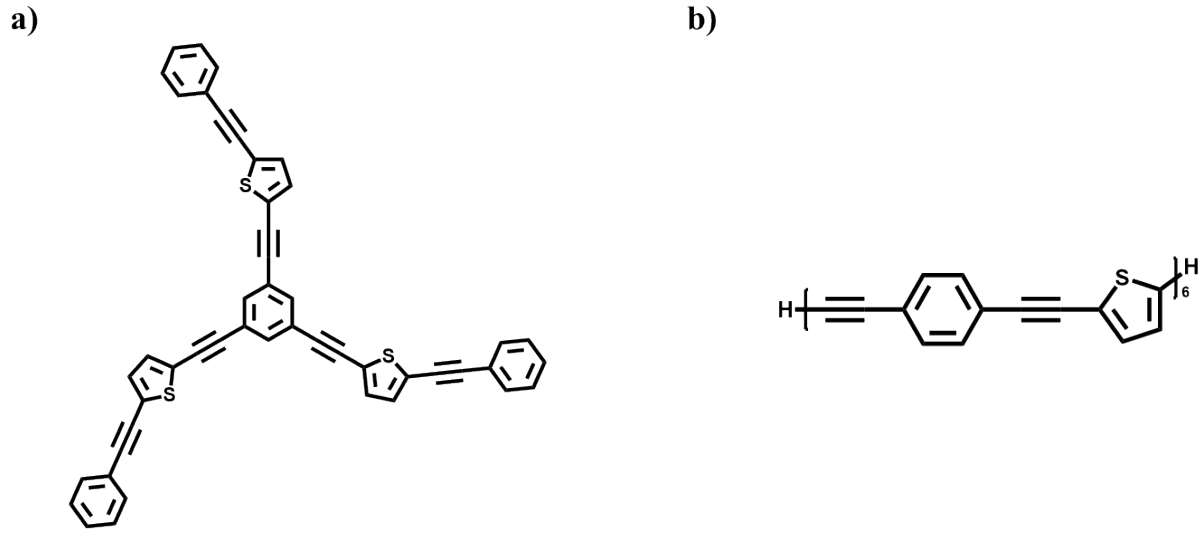

Figure S48: Simulation models of polymers (a) TE1 and (b) DE1.

For each of the TE polymers, the simulation model consisted of a single unit of monomer 1 substituted with three units of monomer 2. The latter were capped by phenylacetylene (–C≡C–C_6H_5) groups. In Figure S48a, the resulting model is shown on the example of polymer TE1. The DE polymers, in turn, were each represented by an oligomer which consists of six repeat units (see Figure S48b). The termini of the oligomer chain were capped with hydrogen atoms.

The structures of the oligomers were constructed with the program STK.[2] Afterwards, for each oligomer, we generated a set of 500 trial structures to serve as the starting points for the conformation search. These were sampled from molecular dynamics (MD) trajectories in which the electronic structure of the oligomer was treated with the use of the extended semiempirical tight-binding[3] (xTB) model. In order to allow the oligomer to sample a broad volume of the conformation space, during the MD simulations the temperature of the system was maintained at 600 K. Afterwards, the trial structures were optimized at the xTB level of theory.

The resulting equilibrium geometries were ranked according to energy. It was assumed that the lowest-energy conformer of each oligomer is representative of the properties of the given polymer. Accordingly, this conformer was selected for the calculation of the electronic and optical properties.

The xTB calculations were performed with the Semiempirical Extended Tight-Binding Program Package (xtb2019), version 5.6.4SE, and used the GFN2 parameterization of the xTB

model.[4] Aqueous solvation was represented via the generalized Born model augmented with the hydrophobic solvent accessible surface area term (GBSA). At the stage of the conformation search, all oligomers were considered to exist in the charge-neutral forms.

Table S7: DFT Calculations of EA and IP of TE1-12 and DE1-12.

TE-n Polymer	IP / V	EA / V	DE-n Polymer	IP / V	EA / V
TE1	0.924	-1.877	**DE1**	0.674	-1.588
TE2	0.668	-1.777	**DE2**	0.518	-1.593
TE3	0.504	-1.721	**DE3**	0.411	-1.602
TE4	0.805	-1.847	**DE4**	0.601	-1.593
TE5	1.450	-1.568	**DE5**	1.215	-1.27
TE6	1.491	-1.658	**DE6**	1.262	-1.331
TE7	1.297	-1.839	**DE7**	1.052	-1.533
TE8	1.243	-1.745	**DE8**	1.052	-1.578
TE9	0.908	-2.092	**DE9**	0.739	-1.886
TE10	1.061	-1.992	**DE10**	0.879	-1.79
TE11	1.283	-1.615	**DE11**	1.099	-1.464
TE12	0.890	-2.148	**DE12**	0.72	-1.94

2.12 Hydrogen evolution experiments

Table S8: High-throughput hydrogen evolution performance of TE1-12 and DE1-12.

TE-n Polymer	Hydrogen evolution[a] / µmol g^{-1} h^{-1}	DE-n Polymer	Hydrogen evolution[a] / µmol g^{-1} h^{-1}
TE1	49.7	**DE1**	149.5
TE2	21.3	**DE2**	77.4
TE3	46.4	**DE3**	90.9
TE4	45.2	**DE4**	77.0
TE5	263.4	**DE5**	115.0
TE6	21.2	**DE6**	298.7
TE7	29.9	**DE7**	131.8
TE8	219.1	**DE8**	247.5
TE9	47.1	**DE9**	225.6
TE10	24.3	**DE10**	37.9
TE11	1811.0	**DE11**	1565.7
TE12	28.4	**DE12**	235.7

[a] 5 mg polymer with 3 wt.% Pt were dispersed in 5 mL triethylamine/methanol/water (1:1:1) mixture, irradiated by a solar simulator (AM1.5G, Class AAA, IEC/JIS/ASTM, 1440 W Xe, 12 × 12 in., MODEL: 94123A, illumination time: 2 hours).

2.13 Correlation of measurements with observed hydrogen evolution rates

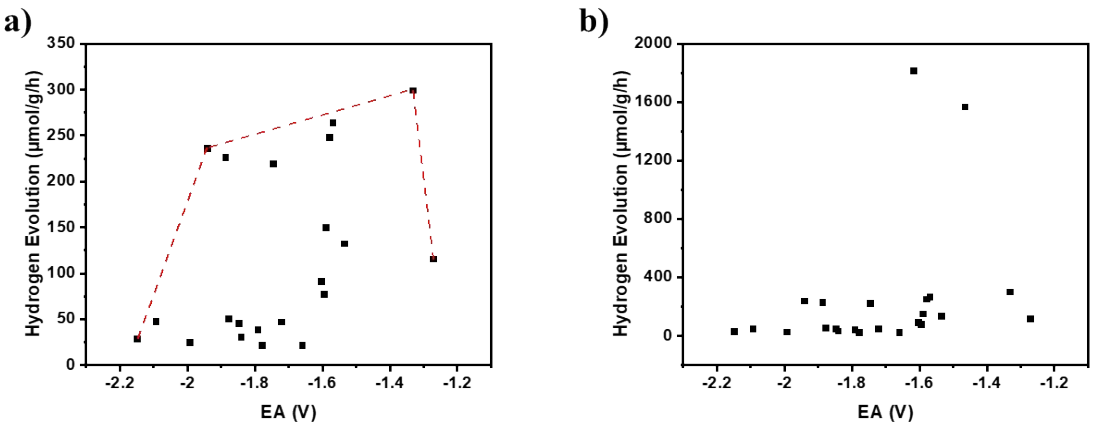

Figure S49: Comparison of the predicted EA to the hydrogen evolution rates of a) except for TE11 and DE11, b) all TE and DE polymers.

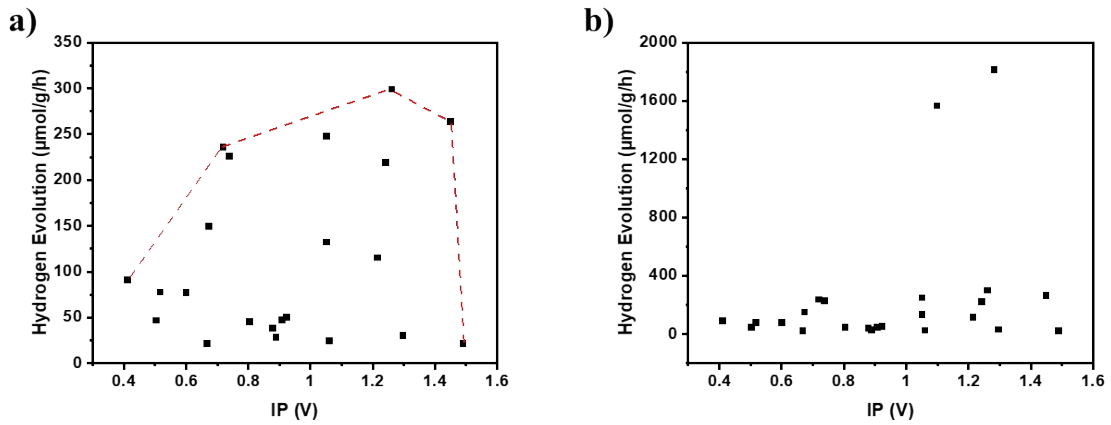

Figure S50: Comparison of the predicted IP to the hydrogen evolution rates of a) except for TE11 and DE11, b) all TE and DE polymers.

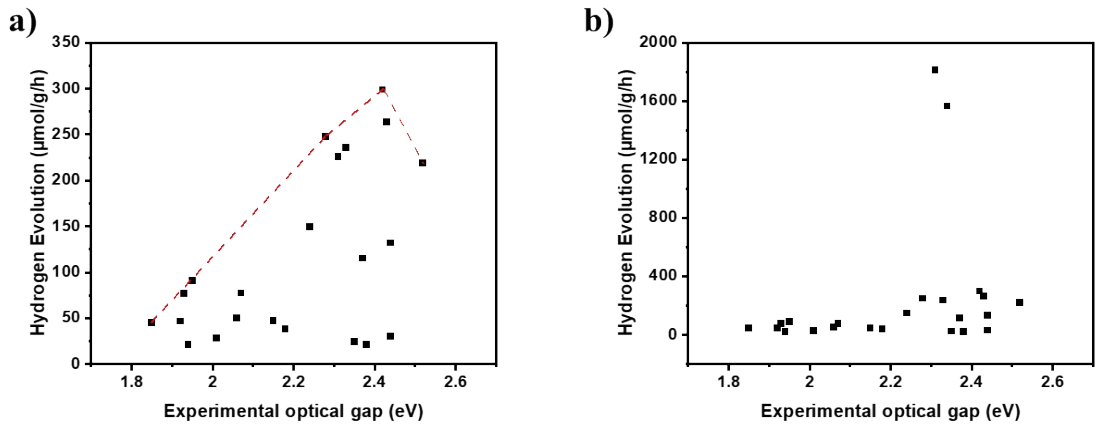

Figure S51: Comparison of the experimental optical gap to the hydrogen evolution rates of a) except for TE11 and DE11, b) all TE and DE polymers.

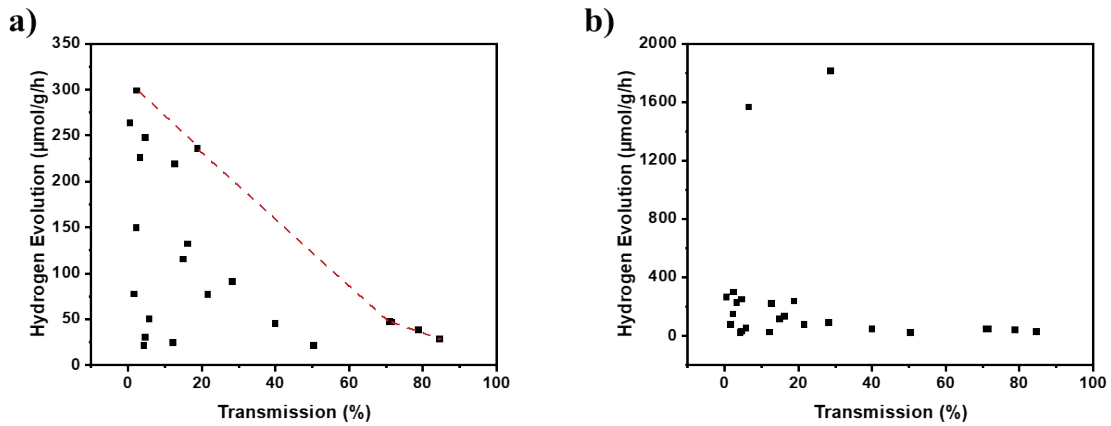

Figure S52: Comparison of the light transmittance to the hydrogen evolution rates of a) except for TE11 and DE11, b) all TE and DE polymers.

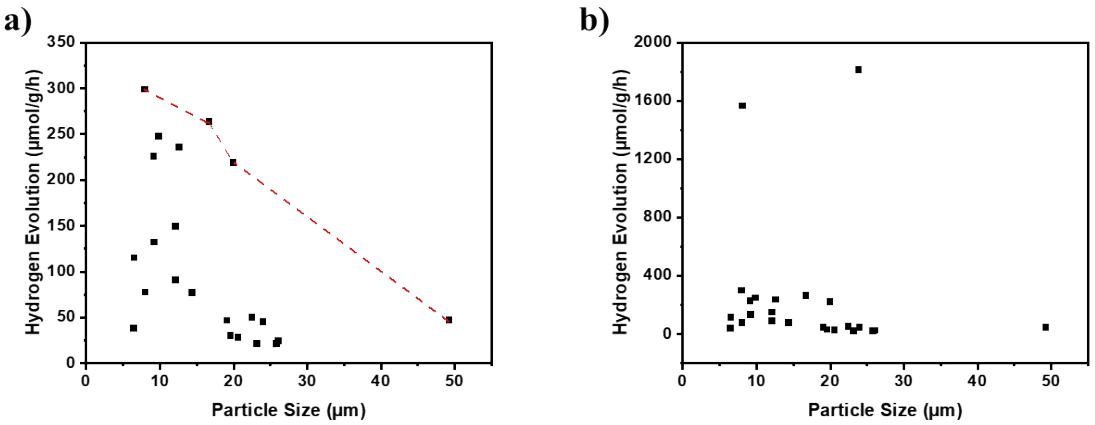

Figure S53: Comparison of the particle size (measured in static light scattering experiments) to the hydrogen evolution rates of a) except for TE11 and DE11, b) all TE and DE polymers.

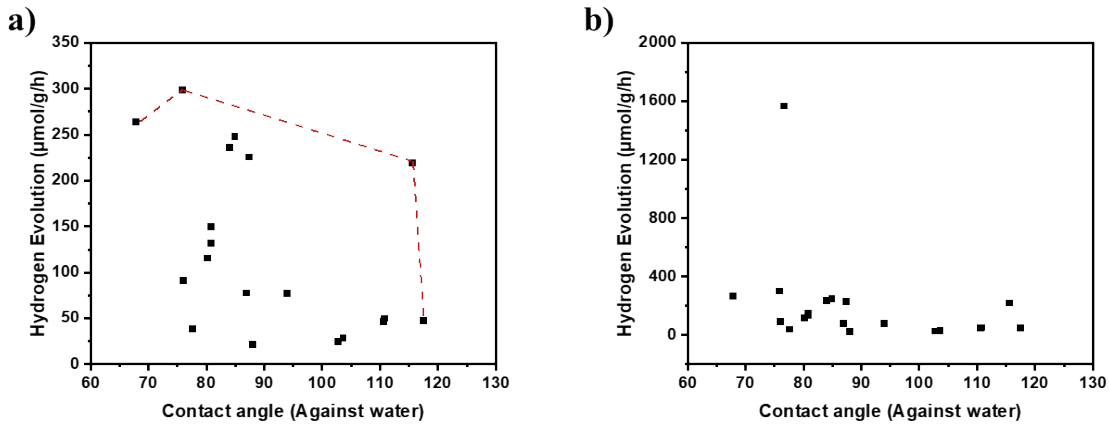

Figure S54: Comparison of the contact angle to the hydrogen evolution rates of a) except for swelling samples and DE11, b) except for swelling samples (TE4, TE6, TE7 and TE11).

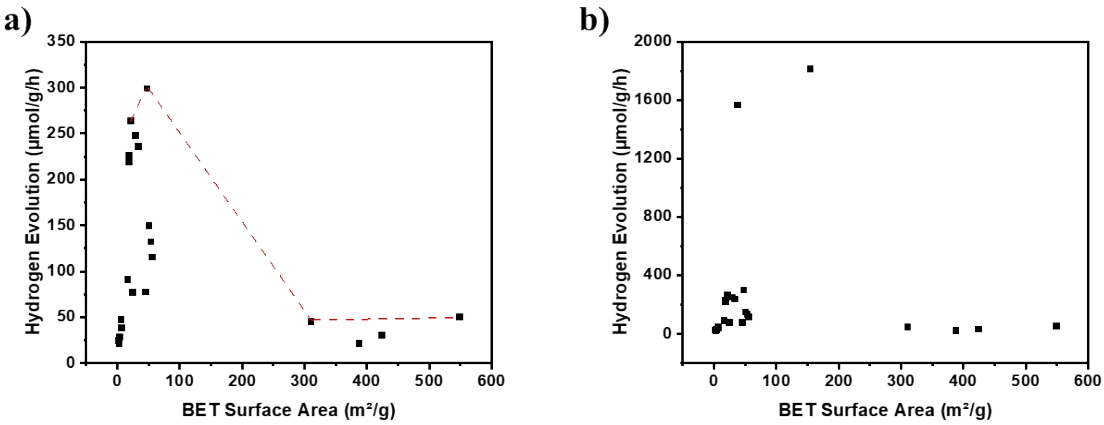

Figure S55: Comparison of the surface area (SA_{BET}, N_2) to the hydrogen evolution rates of a) except for TE11 and DE11, b) all TE and DE polymers.

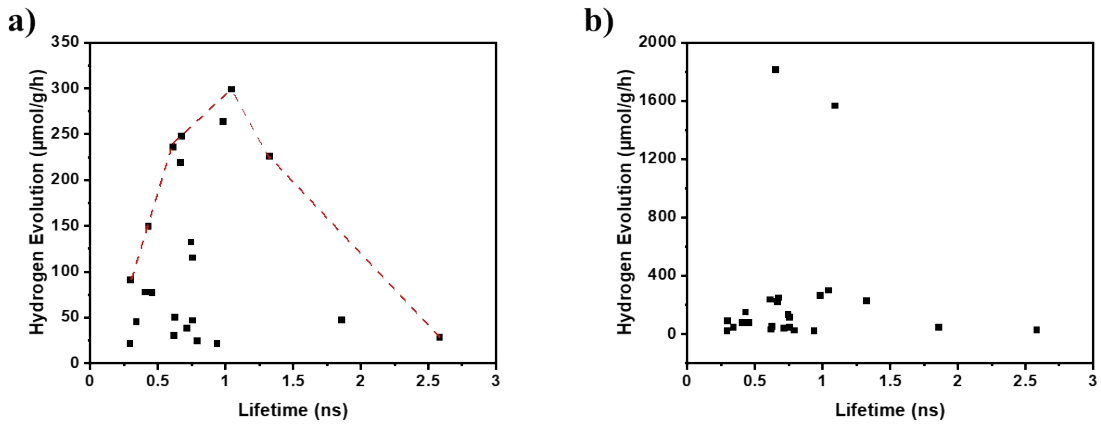

Figure S56: Comparison of the averaged fluorescence lifetime to the hydrogen evolution rates of a) except for TE11 and DE11, b) all TE and DE polymers.

2.14 Characterization of TE11, TEB11 and TEBN11

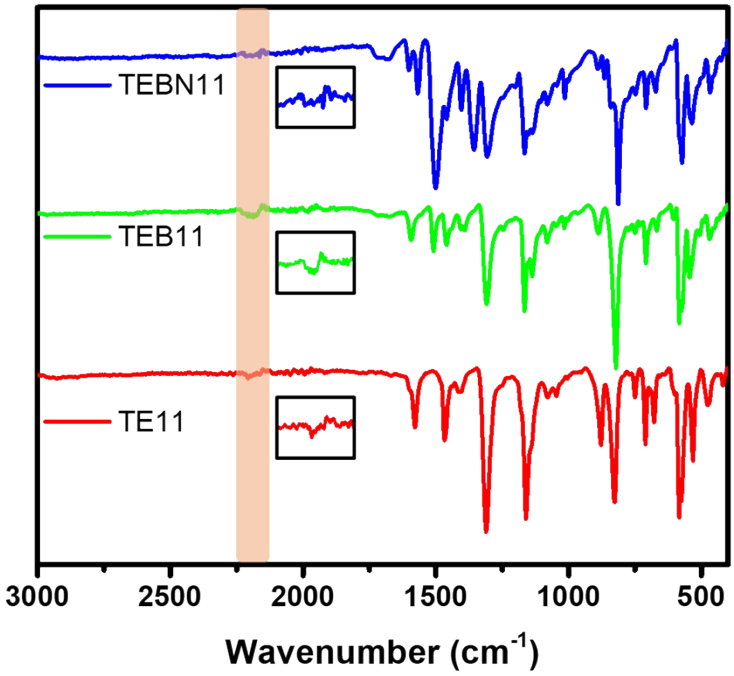

Figure S57: Fourier-transform infrared spectroscopy of TE11, TEB11 and TEBN11.

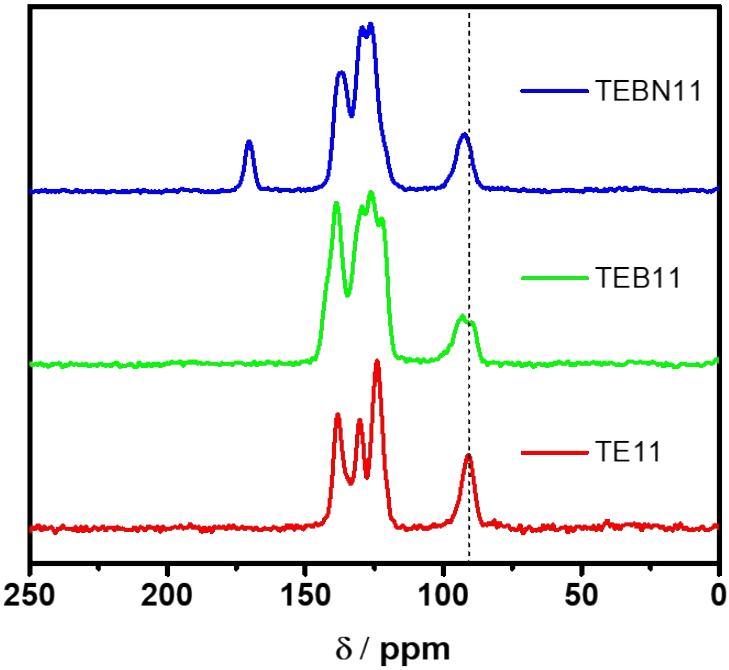

Figure S58: Solid-state ^{13}C NMR spectra of TE11, TEB11 and TEBN11.

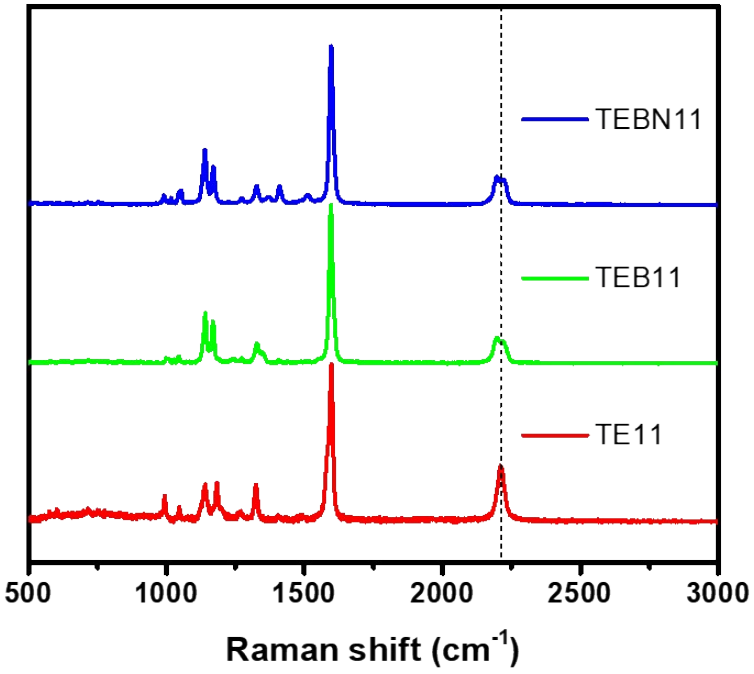

Figure S59: Raman spectra of TE11, TEB11 and TEBN11.

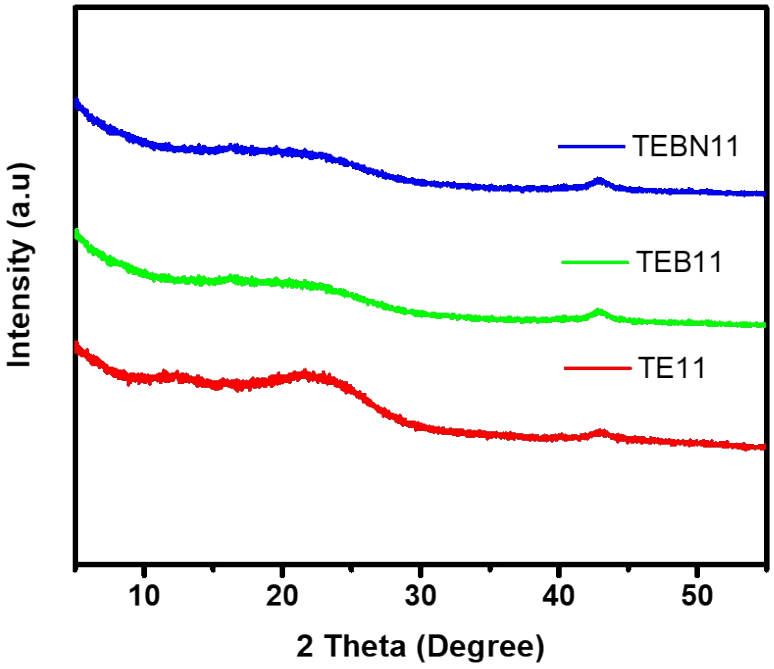

Figure S60: PXRD patterns of TE11, TEB11 and TEBN11.

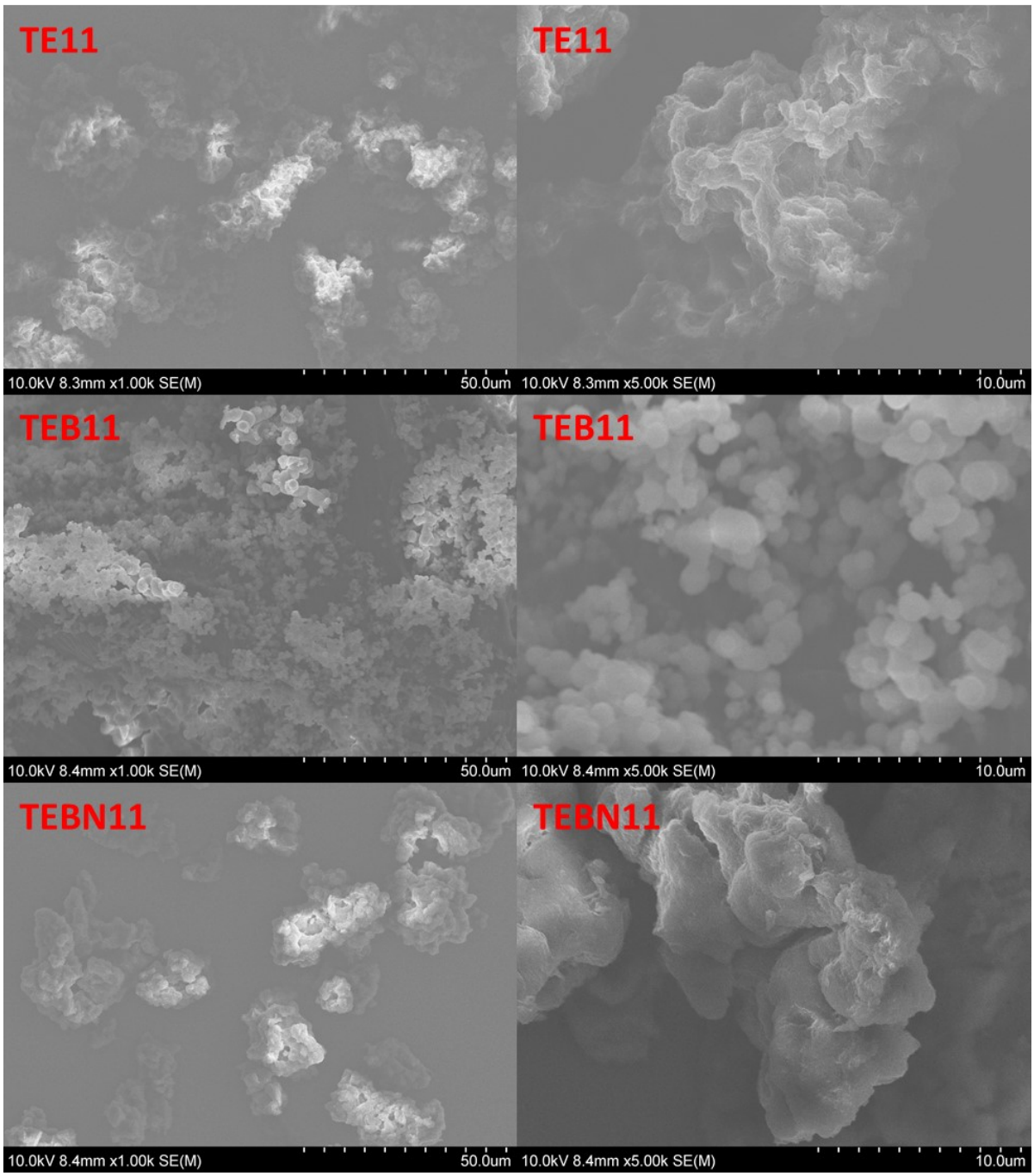

Figure S61: SEM images of TE11, TEB11 and TEBN11.

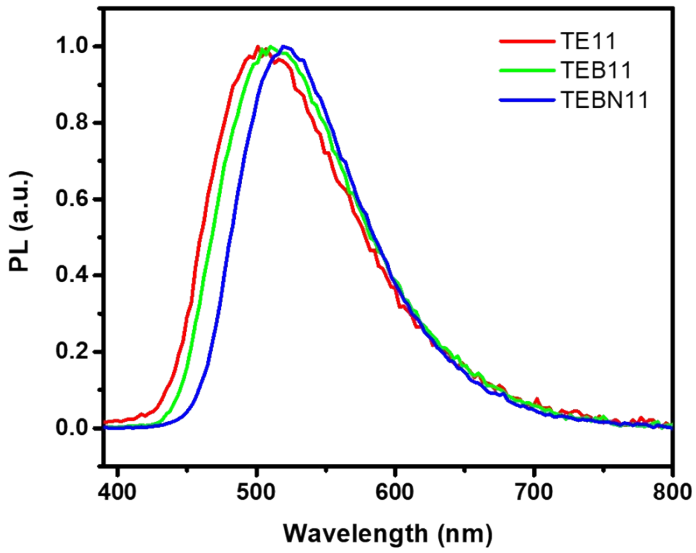

Figure S62: Photoluminescence emission spectra (λ_{exc} = 371 nm) of TE11, TEB11 and TEBN11.

Table S9: Estimated fluorescence lifetimes of TE11, TEB11 and TEBN11.

Polymer	**λem / nm**	**τ_1 / ns**	**B_1 / %**	**τ_2 / ns**	**B_2 / %**	**τ_3 / ns**	**B_3 / %**	**χ^2**	**τ_{avg}[a] / ns**
TE11	500	0.20	53.21	0.78	40.51	3.68	6.28	1.531	0.66
TEB11	510	0.28	52.72	0.99	40.50	3.81	6.78	1.281	0.80
TEBN11	520	0.53	34.56	1.40	44.08	3.52	21.36	1.487	1.55

[a] Fluorescence lifetimes for all polymers obtained from fitting time-correlated single photon counting decays to a sum of three exponentials, which yield τ_1, τ_2, and τ_3 according $\sum_{i=1}^{n}(A + B_i exp(-t/\tau_i))$. τ_{avg} is the weighted average lifetime calculated as $\sum_{i=1}^{n}(B_i\tau_i)$.

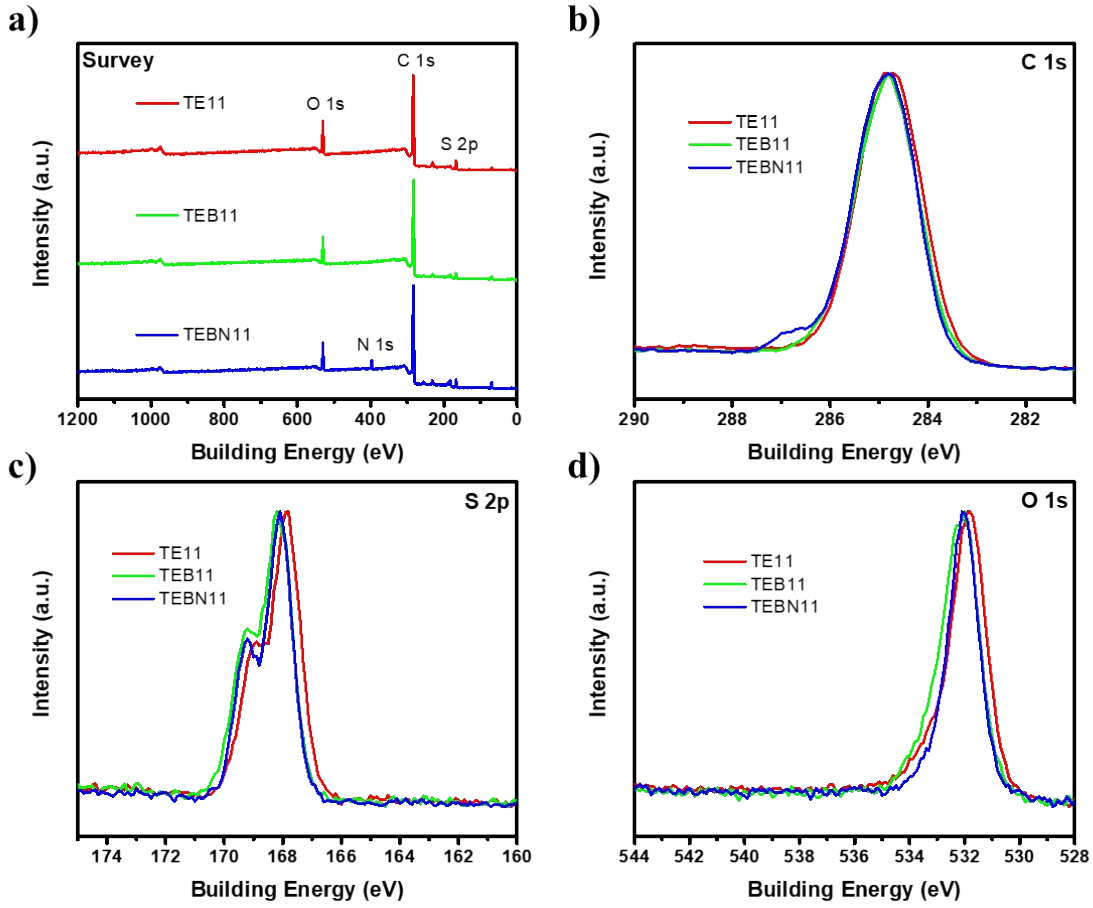

Figure S63: XPS spectra of TE11, TEB11 and TEBN11: a) survey spectra, high resolution spectra of b) C 1s, c) S 2p and d) O 1s.

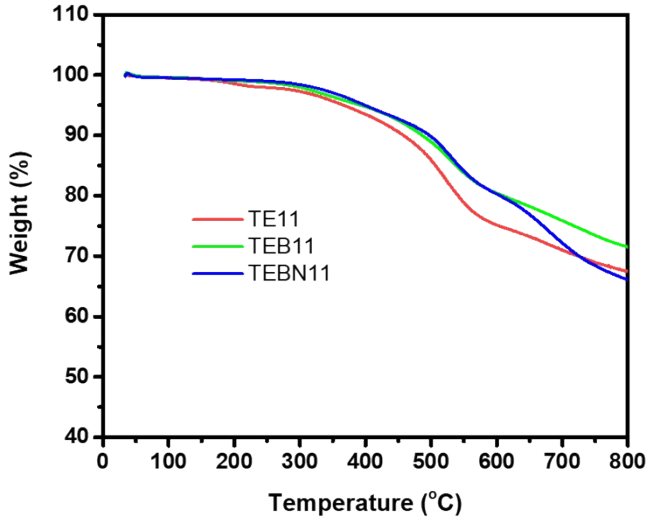

Figure S64: Thermogravimetric data of TE11, TEB11 and TEBN11.

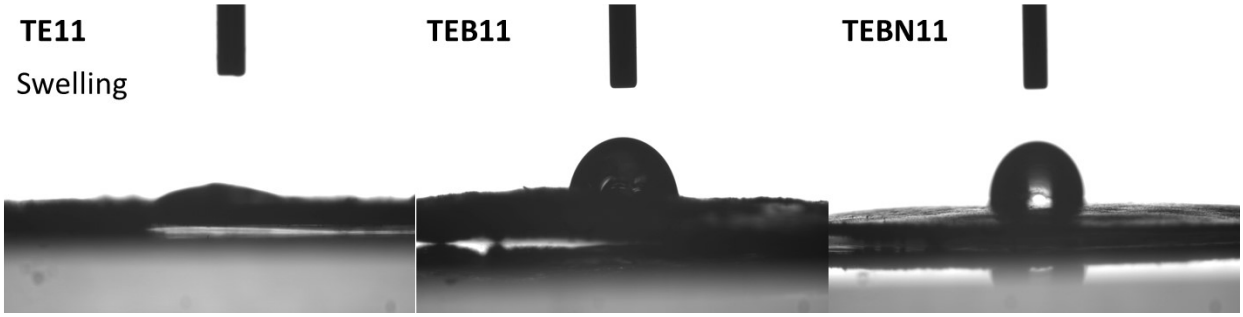

Figure S65: Contact angle images against water of TE11, TEB11 and TEBN11. For swelling polymer TE11, the image is taken several seconds after the drop is deposited onto the polymer surface.

Table S10: Transmission, BET, contact angle and HER of TE11, TEB11 and TEBN11.

Polymer	Transmission TEA/MeOH/H_2O / %	Surface Area[a] / $m^2\ g^{-1}$	Contact angle against water / °	HER[b] / $\mu mol\ g^{-1}\ h^{-1}$	HER[c] / $\mu mol\ g^{-1}\ h^{-1}$	HER[d] / $\mu mol\ g^{-1}\ h^{-1}$
TE11	22.7	154.9	Swelling	1714.8	1811.0	1080±41
TEB11	7.3	12.8	81.3 (±2.0)	1983.8	2103.2	1186±131
TEBN11	17.9	13.6	94.8 (±2.0)	2664.1	3288.5	1894±258

[a] BET Surface area determined from the absorption branch of the absorption isotherm measured at 77 K.

[b] 5 mg polymer without Pt in 5 mL TEA/MeOH/H_2O mixture under a solar simulator (AM1.5G, Class AAA, IEC/JIS/ASTM, 1440 W Xe, 12 × 12 in., MODEL: 94123A, illumination time: 2 hours).

[c] 5 mg polymer with 3 wt. % Pt in 5 mL TEA/MeOH/H_2O mixture under a solar simulator (AM1.5G, Class AAA, IEC/JIS/ASTM, 1440 W Xe, 12 × 12 in., MODEL: 94123A, illumination time: 2 hours).

[d] 25 mg polymer with 3 wt. % Pt in 25 mL TEA/MeOH/H_2O mixture under visible light illumination (300 W Xe light with a $\lambda > 420$ nm filter).

Table S11: Pt content of TE11, TEB11 and TEBN11.

Polymer	Added Pt before photoreaction[a] / wt. %	Detected Pt after photoreaction[b] / wt. %
TE11	3.0	1.2
TEB11	3.0	0.8
TEBN11	3.0	1.1

[a] The amount was calculated based on the assumption that full deposition of the H_2PtCl_6 precursor occurs.

[b] The amount was determined vis ICP-OES measurements.

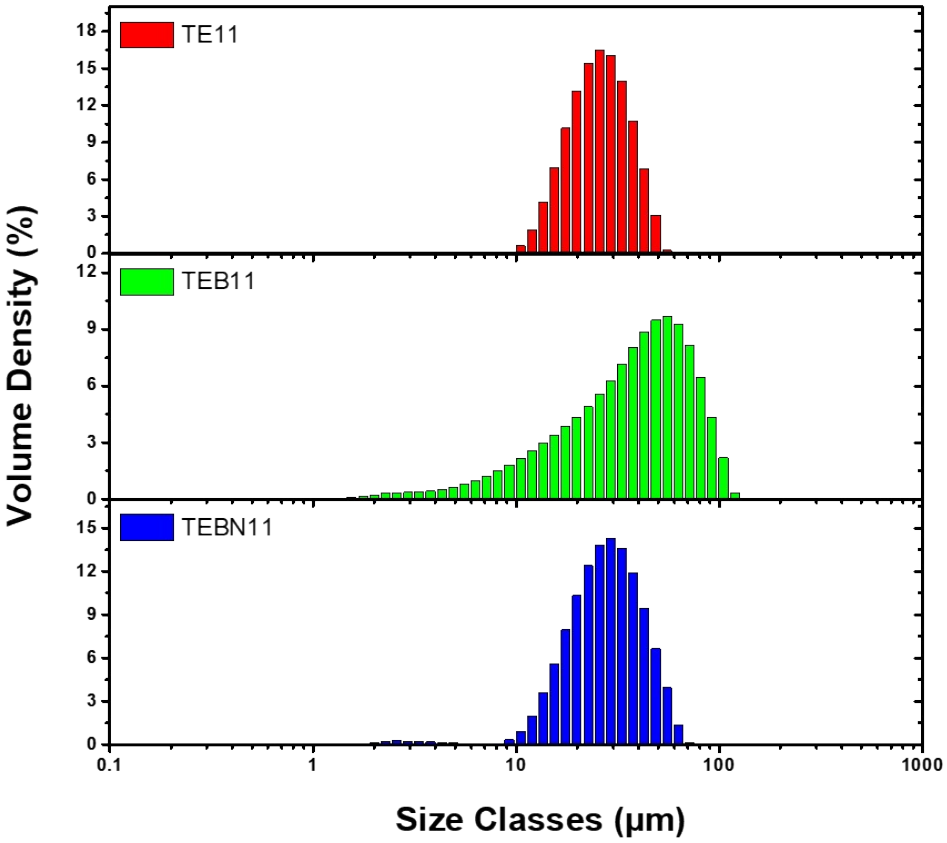

Figure S66: Static light scattering experiments of TE11, TEB11 and TEBN11.

Table S12: Particle sizes by static light scattering of TE11, TEB11 and TEBN11.

Polymer	*D*x50[a] / µm	*D*[4,3][b] / µm	*D*[3,2][c] / µm	Relative external surface area[d] / m^2 kg^{-1}
TE11	25.5	26.7	23.9	251.5
TEB11	39.5	42.2	22.3	268.8
TEBN11	27.7	29.2	22.8	262.8

[a] 50th Percentile of particle size volume distribution; [b] Volume mean diameter; [c] Surface area mean diameter (Sauter mean diameter);[1] [d] Relative extrinsic surface area calculated by dividing the total surface area of the particles by the total mass, assuming a density of 1 g cm^{-3}.

2.15 Photoelectrochemical measurements of TE11, TEB11 and TEBN11

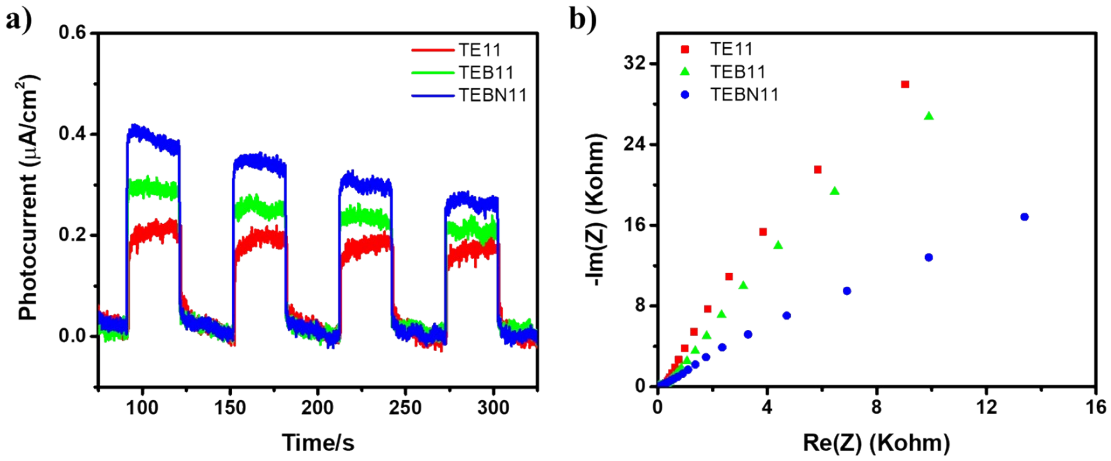

Figure S67: a) Photocurrent densities vs. time for TE11, TEB11 and TEBN11 with applied potentials at 0.6 V vs. Ag/AgCl under intermittent irradiation. b) EIS Nyquist plots of TE11, TEB11 and TEBN11 at a voltage of 0.6 V vs. Ag/AgCl.

2.16 Stability of TEBN11

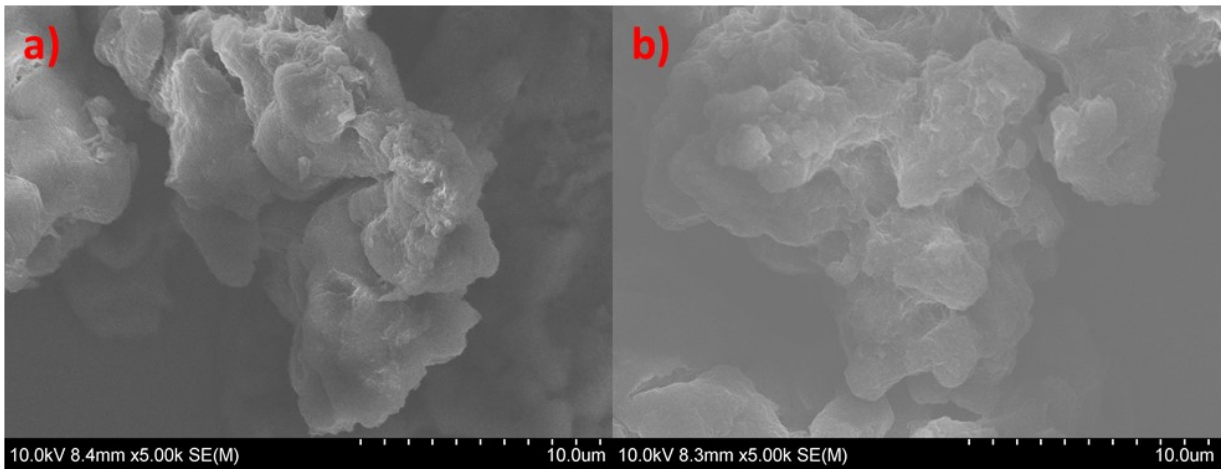

Figure S68: SEM images of TEBN11 a) Before photocatalytic H_2 evolution reaction and b) After photocatalytic H_2 evolution reaction.

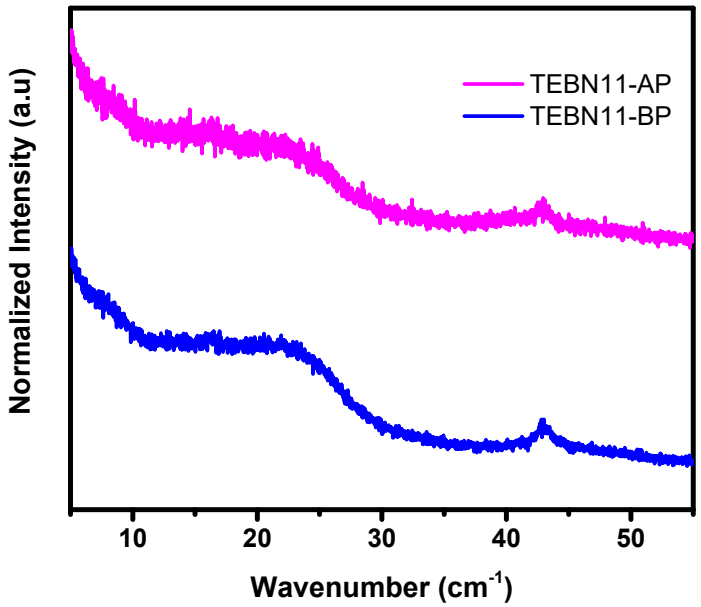

Figure S69: PXRD patterns of TEBN11 before photocatalytic H_2 evolution reaction (BP, blue line) and after photocatalytic H_2 evolution reaction (AP, pink line).

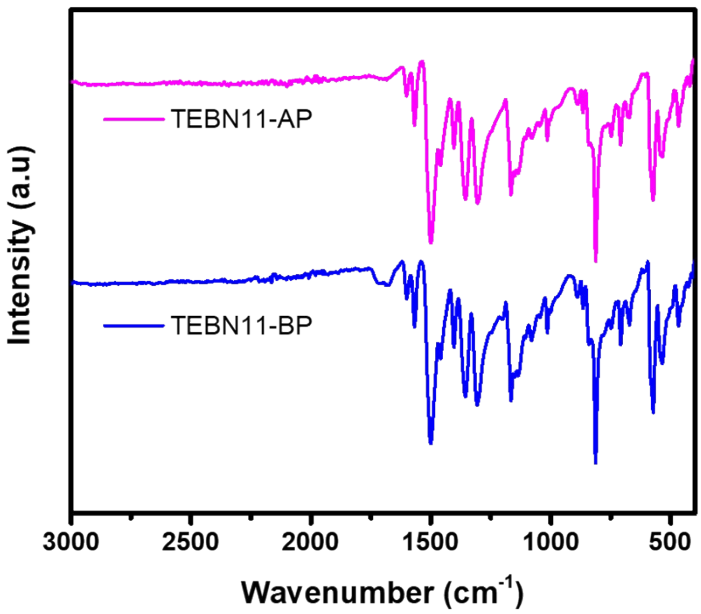

Figure S70: Fourier-transform infrared spectroscopy of TEBN11 before photocatalytic hydrogen evolution reaction (BP, blue line) and after photocatalytic hydrogen evolution reaction (AP, pink line).

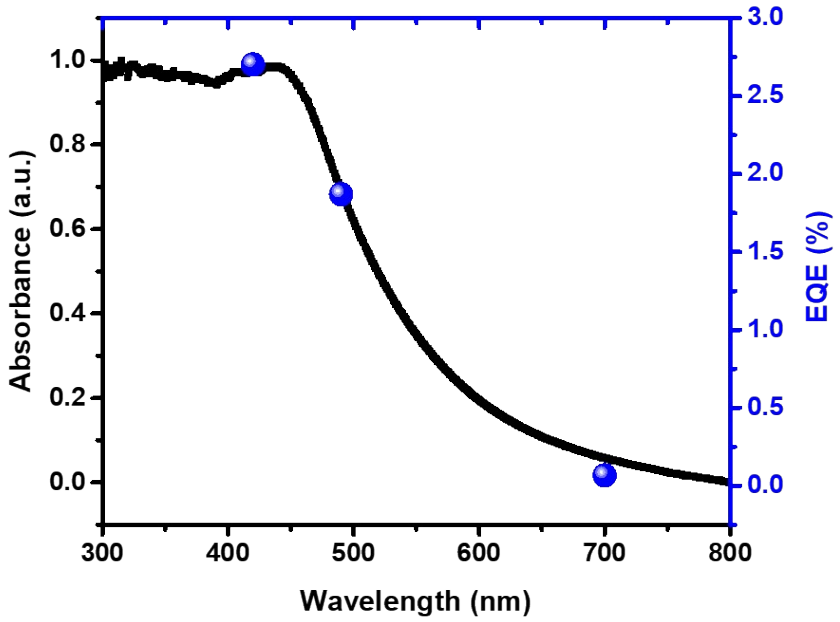

Figure S71: Wavelength dependent external quantum efficiency (EQE) values and solid UV-vis spectrum of TEBN11, λ = 420, 490, 700 nm.

Table S13: Comparation of TEBN11 with recent representative organic polymer photocatalysts for photocatalytic H_2 evolution.

Sample	Co-catalyst	Reaction solution[a]	λ / nm	EQE / %	Ref.
TEBN11	3 wt.% Pt	TEA/MeOH/H_2O	420	2.7	**This work**
TEBN11	3 wt.% Pt	TEA/MeOH/H_2O	490	1.9	**This work**
TEBN11	3 wt.% Pt	TEA/MeOH/H_2O	700	0.1	**This work**
TEB11	3 wt.% Pt	TEA/MeOH/H_2O	420	1.6	**This work**
TE11	3 wt.% Pt	TEA/MeOH/H_2O	420	1.6	**This work**
P7	Pd residue	TEA/MeOH/H_2O	420	7.2	[5]
P10	Pd residue	TEA/MeOH/H_2O	420	11.6	[6]
P64	Pd residue	TEA/MeOH/H_2O	420	20.7	[7]
CTF-2	3 wt.% Pt	TEA/MeOH/H_2O	420	1.6	[8]
OB-POP-3	3 wt.% Pt	TEOA/H_2O	420	2.0	[9]
N_3-COF	0.68 wt.% Pt	TEOA/PBS buffer	450	0.44	[10]
PCP_{4e}	2 wt.% Pt	TEA/H_2O	350	1.8	[11]
2DPCN	3 wt.% Pt	TEOA/H_2O	490	1.3	[12]
TFPT-OCH_3	3 wt.% Pt	TEOA/H_2O	405	1.03	[13]
NCQDs/PFTBTA Pdot	-	DEA/H_2O	420	0.56	[14]
TP-BDDA	3 wt.% Pt	TEOA/H_2O	420	1.3	[15]

[a] TEA: triethylamine, DEA: diethylamine, MeOH: methanol, TEOA: triethanolamine, PBS: phosphate buffered saline.

References

1. A. R. Jones, *Prog. Energy Combust. Sci.*, 1999, **25**, 1-53.
2. L. Turcani, E. Berardo and K. E. Jelfs, *J. Comput. Chem.*, 2018, **39**, 1931-1942.
3. S. Grimme, C. Bannwarth and P. Shushkov, *J. Chem. Theory Comput.*, 2017, **13**, 1989-2009.
4. C. Bannwarth, S. Ehlert and S. Grimme, *J. Chem. Theory Comput.*, 2019, **15**, 1652-1671.
5. R. S. Sprick, B. Bonillo, R. Clowes, P. Guiglion, N. J. Brownbill, B. J. Slater, F. Blanc, M. A. Zwijnenburg, D. J. Adams and A. I. Cooper, *Angew. Chem. Int. Ed.*, 2016, **55**, 1792-1796.
6. M. Sachs, R. S. Sprick, D. Pearce, S. A. J. Hillman, A. Monti, A. A. Y. Guilbert, N. J. Brownbill, S. Dimitrov, X. Shi, F. Blanc, M. A. Zwijnenburg, J. Nelson, J. R. Durrant and A. I. Cooper, *Nat. Commun.*, 2018, **9**, 4968.
7. Y. Bai, L. Wilbraham, B. J. Slater, M. A. Zwijnenburg, R. S. Sprick and A. I. Cooper, *J. Am. Chem. Soc.*, 2019, **141**, 9063-9071.
8. C. B. Meier, R. S. Sprick, A. Monti, P. Guiglion, J.-S. M. Lee, M. A. Zwijnenburg and A. I. Cooper, *Polymer*, 2017, **126**, 283-290.
9. S. Bi, Z.-A. Lan, S. Paasch, W. Zhang, Y. He, C. Zhang, F. Liu, D. Wu, X. Zhuang, E. Brunner, X. Wang and F. Zhang, *Adv. Funct. Mater.*, 2017, **27**, 1703146.
10. V. S. Vyas, F. Haase, L. Stegbauer, G. Savasci, F. Podjaski, C. Ochsenfeld and B. V. Lotsch, *Nat. Commun.*, 2015, **6**, 8508.
11. L. Li, Z. Cai, Q. Wu, W.-Y. Lo, N. Zhang, L. X. Chen and L. Yu, *J. Am. Chem. Soc.*, 2016, **138**, 7681-7686.
12. L. Zhang, N. Ding, J. Wu, K. Iwasaki, L. Lin, Y. Yamaguchi, Y. Shibayama, J. Shi, H. Wu, Y. Luo, K. Nakata, D. Li, X. Wang, A. Fujishima and Q. Meng, *Catal. Sci. Technol.*, 2018, **8**, 3846-3852.
13. K. Yu, S. Bi, W. Ming, W. Wei, Y. Zhang, J. Xu, P. Qiang, F. Qiu, D. Wu and F. Zhang, *Polym. Chem.*, 2019, **10**, 3758-3763.
14. M. H. Elsayed, J. Jayakumar, M. Abdellah, T. H. Mansoure, K. Zheng, A. M. Elewa, C.-L. Chang, L.-Y. Ting, W.-C. Lin, H.-h. Yu, W.-H. Wang, C.-C. Chung and H.-H. Chou, *Appl. Catal. B-Environ.*, 2021, **283**, 119659.
15. P. Pachfule, A. Acharjya, J. Roeser, T. Langenhahn, M. Schwarze, R. Schomäcker, A. Thomas and J. Schmidt, *J. Am. Chem. Soc.*, 2018, **140**, 1423-1427.